



Sediment distribution and sedimentary processes across the Antarctic Wilkes Land margin during the Quaternary

C. Escutia^{a,*}, D. Warnke^b, G.D. Acton^c, A. Barcena^d, L. Burckle^e,
M. Canals^f, C.S. Frazee^b

^a*Instituto Andaluz de Ciencias de la Tierra CSIC/Universidad de Granada Facultad de Ciencias Campus de Fuentenueva s/n 18002 Granada, Spain*

^b*California State University, Hayward, CA 94542-3088, USA*

^c*Ocean Drilling Program, Texas A&M University, College Station, TX 77845, USA*

^d*Universidad de Salamanca, Facultad de Ciencias, 37008-Salamanca, Mexico*

^e*Lamont Doherty Earth Observatory, Palisades, New York 10964, USA*

^f*Universidad de Barcelona, E-08028 Barcelona, Spain*

Abstract

The study of existing cores collected across the Wilkes Land margin provides us with a better understanding of the sediment distribution and processes across this margin during the Holocene, and during Pleistocene glacial and interglacial cycles. Holocene depositional rates are high in deep (> 1000 m) inner-shelf basins where diatomaceous ooze is deposited at estimated minimum sedimentation rates ranging from 40 to 60 cm/kyr. In the shelf troughs, Holocene sediment has a patchy distribution or is totally absent. This is also the case on the shelf banks due to differential deposition because of the irregular relief of the continental shelf and the erosion and redistribution by bottom currents. Pleistocene *interglacial* sedimentation is well represented in sediment from the continental rise and is dominated by hemipelagic deposition of massive mud with the highest biogenic content (as indicated by %opal) and with a high abundance of clasts (IRD). During the Pleistocene *glacial* cycles, diamictons were deposited in the continental-shelf troughs and on the banks. Reworking (e.g., by bottom currents) and remobilization (e.g., gravity flows) of these diamictons is a common process along the shallow continental-shelf banks. On the continental slope and the continental rise, gravity flows are one of the most important sedimentary processes. Sediment from continental-slope cores, with a texture that greatly resembles the diamictons on the shelf, is interpreted to represent either part of a slump block or the start of a debris flow. Downslope, crudely stratified to laminated intervals represent the transition between an end member of a debris flow and a turbidity flow. Some of the laminated intervals in cores from the continental rise represent sediment deposited from a turbidity flow. Ages obtained from cores further support that slumps and gravity flows are dominant processes in this margin, because numerous hiatuses apparently are present in cores from the base of the slope. One of these cores extends into the Miocene. Elsewhere on the continental rise, massive and laminated sediments in cores of similar length record near-continuous Pleistocene sedimentation.

© 2003 Elsevier Science Ltd. All rights reserved.

1. Introduction

Sediment deposited on the Wilkes Land continental shelf, slope, and rise during Cenozoic time

*Corresponding author.

E-mail address: cescutia@ugr.es (C. Escutia).

hold a record of the history of glacial advance and retreat across this segment of the East Antarctic margin. The current stratigraphic model for this margin is derived from various studies of the continental shelf, slope, and rise. Episodes of ice advance produced erosional surfaces and over-compacted sediment both in shelf troughs and on banks, as well as steeply prograded wedges on the outer continental-shelf troughs and upper slope (Eittrheim and Smith, 1987; Wannesson, 1991; Tanahashi et al., 1994; Eittrheim et al., 1995). The large volume of unconsolidated and unsorted material brought to the outer shelf and slope by the ice streams must cause slope instability and the generation of turbidity currents. On the continental rise, these turbidity currents develop the channel and levee complexes characteristic of deep-sea fans (Eittrheim and Smith, 1987; Hampton et al., 1987a,b; Escutia et al., 1997, 2000). Fine-grained overbank sediment became entrained in bottom contour currents and deposited in sediment ridges up to 470 m in relief relative to the surrounding seafloor (Escutia et al., 1997, 2000, 2002). During interglacials, the outer shelf, slope, and continental rise receive a rain of hemipelagic sediment as well as ice-rafted debris (IRD), and are subjected to reworking by slumping and/or oceanic currents. During warmer episodes that are still fully glacial onshore, such as the Holocene, most terrigenous sedimentation occurs in front of the grounding line and in inner-shelf basins. As demonstrated by the study of cores from similar shelf settings west of the Antarctic Peninsula (Domack et al., 1993; Leventer et al., 1996; Barcena et al., 1998, 2002) and George V Coast on the Wilkes Land margin (Presti et al., 2001), these inner-shelf basins effectively trap the products of biogenic productivity.

The above model is based mainly on the interpretation of multichannel seismic profiles, and on sediment cores previously collected from this margin by the Deep-Sea Drilling Project (DSDP) at Sites 268 and 269 (Hayes et al., 1975), the USNS Eltanin cruise (Payne and Conolly, 1972), the Deep Freeze 79 cruise (Domack, 1982), and the USGS 1984 cruise (Hampton et al., 1987b) (Fig. 1). Although these sediment cores were previously analyzed in some detail (e.g., grain size,

X-ray radiographs, physical properties, diatom stratigraphy, limited magnetostratigraphic analyses, etc.), only two studies were directed at understanding sedimentation across the margin, from the continental shelf to the lower continental rise (Payne and Conolly, 1972; Hampton et al., 1987a,b). Other sedimentological studies on this margin focused mainly on understanding the sediment distribution and processes on the shelf and the slope (Milam and Anderson, 1981; Anderson et al., 1983; Dunbar et al., 1985; Domack et al., 1989). In the two studies conducted across the margin, comparisons of coeval sedimentation and sedimentary processes during recent glacial/interglacial periods was difficult to establish because the lack of age control in sediment cores, though some level of correlation across the rise and abyssal plain was possible (Payne and Conolly, 1972).

We have re-examined the previously collected piston cores with several goals. First, we wanted to learn as much as possible about the ages and types of sediment as a means of ground-truthing seismic reflection profiles and planning for future proposed drilling for the Integrated Ocean Drilling Program (IODP). Second, we wanted to understand better the relationships between diachronous and coeval processes occurring across the shelf, slope, and rise. Third, we hoped to use the somewhat limited information gained from the piston cores to develop a model for Quaternary sedimentation that could possibly be extended to the deeper unsampled sedimentary units imaged in reflection profiles.

To establish better age-control, we conducted diatom biostratigraphic analyses on some of the previously collected sediment piston cores. The primary aim was to test the potential of the sediment from the Wilkes Land margin to yield relative ages in the light of more recent diatom biostratigraphy for the Southern Ocean (Gersonde et al., 1990; Barron et al., 1991; Gersonde and Barcena, 1998; Censarek and Gersonde, 2002; Zielinski and Gersonde, 2002). Paleomagnetic analyses also were conducted on the existing cores to assess the fidelity of the margin sediment for recording environmental changes as well as for studying geomagnetic field behavior. Previous

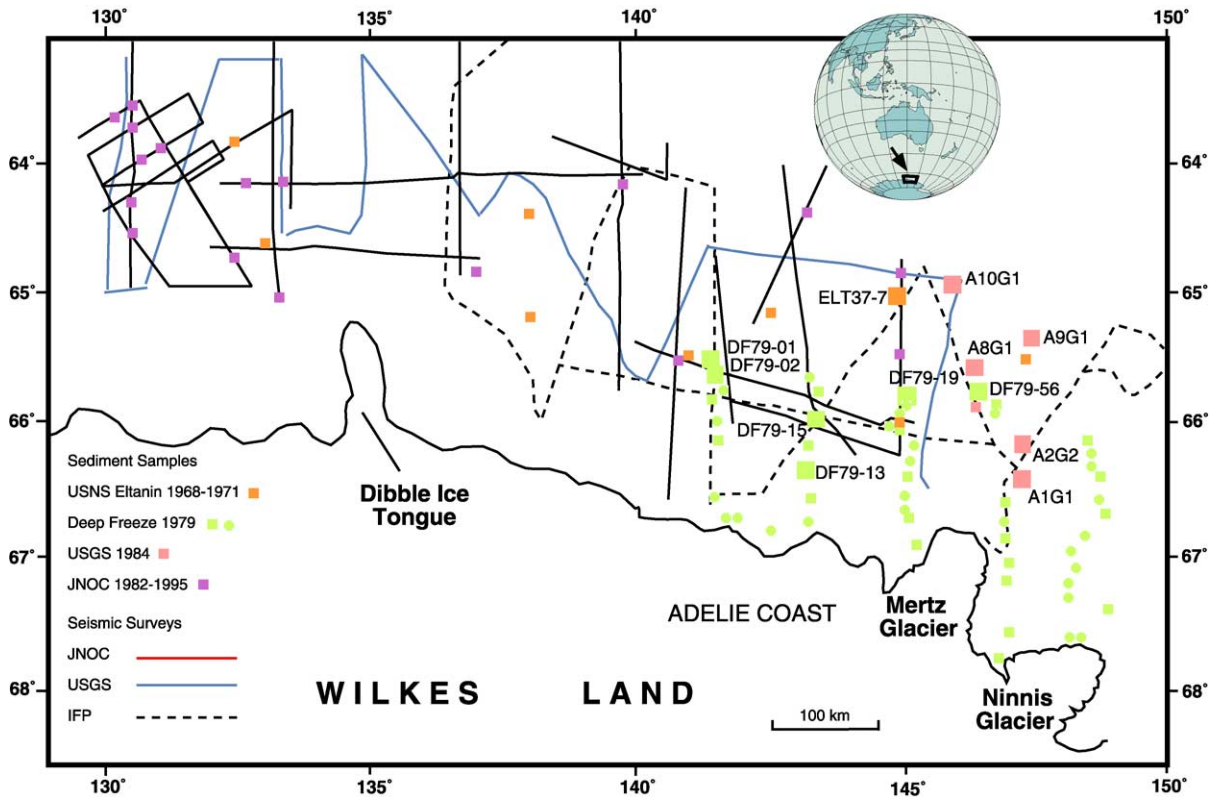


Fig. 1. Map showing the location of multichannel seismic data recorded by the Institut Français du Pétrole (IFP), the Japan National Oil Corporation (JNOC) and the United States Geological Survey (USGS) on the Wilkes Land continental margin. Also shown is the location of sediment cores collected during the USNS Eltanin cruise (Payne and Conolly, 1972), the Deep Freeze 79 cruise (Domack, 1982), and the USGS 1984 cruise (Hampton et al., 1987a,b). Sediment cores analyzed for this study are labeled. Their position with respect to the bathymetry is shown in Figs. 3, 5, 8 and 15.

paleomagnetic analyses on the existing cores were limited to low alternating field (AF) demagnetization of discrete samples (cubes with 6–8 cm³ volumes) from the Eltanin cores (Watkins and Kennett, 1972). Additionally, we conducted biogenic-silica analyses for calibration of downcore magnetic signatures and as a paleoproductivity indicator. Furthermore, clast counts also were conducted at 1-cm intervals to determine whether the clasts were preferentially associated with specific sedimentary facies. Once ages were determined, our goal was to describe and explain Pleistocene and Holocene sediment distribution and sedimentary processes across the Wilkes Land margin during glacial and interglacial periods.

Most of the cores previously collected from this margin before the Italian-Australian WEGA-2000

cruise were examined for this study. Our analyses focus on 12 sediment cores located on the continental shelf, slope, and rise (Table 1, Fig. 1). These cores were selected because they were relatively well preserved and because they sampled the five depositional environments identified across the Wilkes Land margin: inner-shelf basins, erosional shelf troughs, shelf banks, continental slope, and continental rise.

2. Physiographic setting

Fig. 2 shows the general bathymetry of the continental margin off Wilkes Land. The continental shelf is characterized by an irregular topography with: (1) deep (> 1000 m) inner-shelf

Table 1

Location, water depth and length of the sediment cores considered in this study. Also shown are the analyses conducted on samples from these cores

Site	Latitude (°S)	Longitude (°E)	Water depth (m)	Length cored (cm)	Studies conducted			
					Diatom biostrat.	Paleomag.	X-ray (IRD & clast counts)	Opal
DF79-01	65°29'S	141°30'E	2022	558	No	Yes	Yes	Yes
DF79-02	65°34'S	141°34'E	1098	575	No	Yes	Yes	Yes
DF79-13	66°19'S	143°19'E	682	595	Yes	No	No	No
DF79-15	65°52'S	143°20'E	412	359	Yes	No	Yes	No
DF79-19	65°47'S	145°12'E	2598	589	Yes	Yes	Yes	No
DF79-56	65°42'S	146°31'E	2361	255	No	No	Yes	No
ELT37-07	65°00'S	145°00'E	3155	844	No	No	Yes	Yes
USGS A1G1	66°35.3'S	147°21.7'E	611	283	Yes	Yes	Yes	No
USGS A2G2	66°08'S	147°05'E	458	139	Yes	No	No	No
USGS A8G1	65°34.0'S	146°25.4'E	2635	369	Yes	Yes	No	No
USGS A9G1	65°33.7'S	147°21.6'E	3037	368	yes	No	No	No
USGS A10G1	64°54.3'S	145°59.9'E	3379	375	Yes	No	No	No

basins, their continuation, namely (2) shelf troughs, which shoal as they traverse from the inner-shelf basins (>1000 m) to the outer shelf (500 m), and flanking them, (3) shallow (200–400 m) outer-shelf banks. The continental slope, which extends from the shelf break to about 2000–2500 m water depth is steep (gradients ranging between 1:9 and 1:30), narrow (15 km average) and incised by numerous submarine canyons. Seaward of the slope is the continental rise, also relatively steep (average gradients greater than 1:100 in the upper rise to less than 1:150 in the lower rise) and rugged because of a complex network of tributary-like channels that continue from the slope canyons, the levee systems, and sediment mounds.

3. Geological setting

The Wilkes Land continental margin formed in mid-Jurassic/Cretaceous time during an extensional tectonic episode that separated Australia from Antarctica (Cande and Mutter, 1982; Vevers, 1987). The acoustic basement across the margin consists of block-faulted continental crust, thinned, and intruded transitional crust and

oceanic crust (Eittreim and Smith, 1987; Eittreim, 1994). The acoustic basement is covered by up to 8 km of sediment (Eittreim and Smith, 1987). Post-rift Cenozoic strata are mostly undeformed and are more than 2 km thick across the shelf. A marked intra-Cenozoic erosional surface (unconformity WL2, Tanahashi et al., 1994) across the margin has been interpreted to represent the onset of glaciation on the Wilkes Land margin (Eittreim and Smith, 1987; Tanahashi et al., 1994; Eittreim et al., 1995). “Onset” is here defined as the first arrival of grounded ice sheets on the continental shelf. Strata above unconformity WL2 mostly prograde across the shelf and downlap onto WL2. Unconformity WL2 can be traced seaward into the continental rise deposits, where it marks an increase in turbidite deposition and development of sediment mounds (Escutia et al., 1997, 2000, 2002). The inferred time for the formation of unconformity WL2 is Eocene, on the basis of indirect correlation with DSDP 269 (Eittreim et al., 1995; Wannesson, 1991), as well as a nearby piston core from the continental rise dated Cretaceous to early Eocene (Tanahashi et al., 1994). From the time of the formation of unconformity WL2, the sedimentary history of this margin has been closely

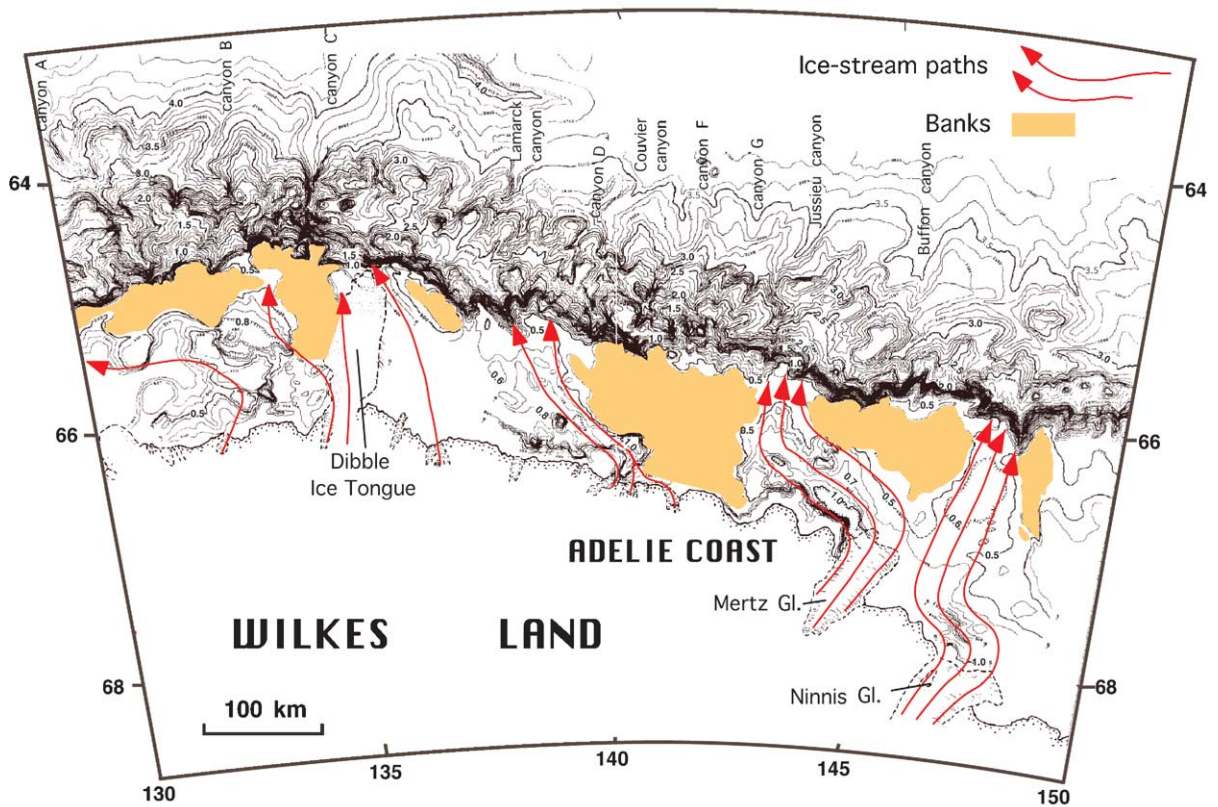


Fig. 2. Wilkes Land bathymetric map modified from Chase et al. (1987) and Eitrem et al. (1995) showing the general physiography of the continental shelf, slope and rise.

related to the glacial history of the adjacent continent.

4. Methodologies

We conducted diatom biostratigraphic, paleomagnetic, and sedimentological analyses following the methodologies described below. Unfortunately, due to the preservation of the sediment cores and/or the lack of enough volume of sample available, we were unable to conduct all analyses on the same core (Table 1).

4.1. Biostratigraphy

Sediment samples were cleaned and prepared on permanent slide mounts for light microscopy according to the method outlined in Barcena and

Abrantes (1998). Absolute diatom numbers were determined from microscope slides with randomly distributed microfossils using a Leica DMLB microscope, in phase contrast and at 1000× magnification. For Cores DF79-13 and DF79-15, counts of more than 400 valves per sample were made using the method of Schrader and Gersonde (1978) (Table 2). For Core DF79-19, in which the number of diatoms per gram was very low, counting 400 or more diatom valves per sample proved too time consuming, so we instead searched for diatoms in more than 400 fields of view for each slide. For USGS Cores A1G1, A2G2, A8G1, A9G1, and A10G1, only those species where more than half the valve was present were counted and about 150–300 individual valves were identified and counted on each slide. The preservation status of the fossil assemblage was estimated by visual examination.

Table 2
Diatom analyses

Depth (cm)	Valves/gram dry sediment	Total counted (RS)	<i>Chaetoceros</i> Taxa	Sea-ice	<i>F. kerguelensis</i>	<i>T. antarctica</i>	<i>E. antarctica</i>	<i>T. lentiginosa</i>	<i>Rhizosolenia</i> sp.
Core DF79-13									
15	3.76E+08	463	110	168	45	10	5		
25	2.21E+08	411	97	185	47	7	1		
38	3.28E+08	433	137	90	94	12	1		
48	7.48E+08	408	191	47	71	9	4		
64	2.66E+08	423	139	84	77	8	8		
74	3.54E+08	557	177	154	75	13	6		
87	2.95E+08	458	130	132	67	12	5		
110	1.89E+08	437	137	92	63	7	8		
132	2.96E+08	417	121	161	34	13	3		
146	2.73E+07	459	100	111	85	10	5		
166	2.09E+08	484	92	193	78	4	5		
186	1.86E+08	363	88	146	50	6	6		
226	2.58E+08	413	128	162	43	11	4		
249	1.96E+08	402	84	113	82	10	7		
273	2.41E+08	528	178	75	72	3	4		
292	3.04E+08	412	55	85	113	9	2		
305	3.12E+08	454	169	72	77	7	2		
325	2.54E+08	415	144	67	63	4	1		
346	1.99E+08	461	52	118	96	19	10		
367	3.93E+08	539	155	121	100	10	5		
387	4.34E+08	375	82	137	70	4	3		
415	1.98E+08	382	56	123	78	6	6		
452	2.62E+08	440	116	74	110	10	3		
492	2.73E+08	509	188	114	87	8	5		
532	1.61E+08	387	35	56	168	10	4		
566	2.72E+08	359	97	67	72	11	6		
582	2.69E+08	391	96	92	90	13	9		
Core DF79-15									
34	1.39E+06	426	68	91	137	7	9	9	11
60	2.70E+06	457	73	86	193	3	15	20	2
80	7.28E+05	411	59	59	205	10	8	24	8
90	1.63E+06	429	102	58	158	0	13	29	8
140	1.67E+06	414	83	60	155	3	12	15	6
178	1.06E+06	402	61	57	184	2	9	25	9
232	1.27E+06	389	75	47	165	2	17	16	9
290	2.92E+06	424	54	39	193	6	10	26	13
338	9.06E+05	410	104	77	139	3	10	11	4

4.2. Paleomagnetism and rock magnetism

We analyzed discrete samples ($\sim 7\text{cm}^3$ of sediment in plastic cubes) and U-channel samples, which are strips of sediment, each $2\text{cm} \times 2\text{cm}$ in

cross section and up to 1.5 m long, collected from the center of split-core sections (Table 1). The samples were collected to assess the paleomagnetic signal, with the goal of determining magnetic polarity where possible, and examining variations

in rock magnetic properties to see if they could be related to environmental changes. The combination of high-latitude and terrigenous sedimentation common to the Antarctic margin have proven exceptional for paleomagnetic studies. For example, ODP Leg 178 continental rise Sites 1095, 1096, and 1101 have yielded possibly the best magnetostratigraphic record ever from high southern latitudes (Barker et al., 1999; Acton et al., 2002).

We focused our attention on the longer, undisturbed, and better preserved cores with fine-grained sediment as these would most likely be viable paleomagnetic recorders and give more continuous records. In some cases, the core had dried completely over long intervals, making U-channel sampling difficult. The upper 279 cm of the archive half of Core DF79-19 was well enough preserved and previously unsampled, so we collected two U-channel samples that spanned the interval. Discrete samples were taken from Cores DF79-01 (13–98 cm at ~15 cm interval), DF79-02 (from 8 to 453 cm at ~20 cm intervals), and DF79-19 (from below the two U-channels at 279 cm to the end of the core at 535 cm at ~20 cm interval), and from Cores USGS A1G1 and A8G8 (from well-preserved core intervals)

Laboratory analysis consisted of (1) natural remanent magnetization (NRM) measurements before and after progressive AF demagnetization up to 70 mT, typically in steps of 5 or 10 mT; (2) low-field magnetic susceptibility measurements; (3) hysteresis properties, including the saturation magnetization (M_s), the saturation remanent magnetization (M_{rs}), the coercivity (H_c), and the coercivity of remanence (H_{cr}); and (4) the acquisition of artificial remanences, including anhysteretic remanent magnetization (ARM) and isothermal remanent magnetization (IRM), and their subsequent progressive AF demagnetization. The ARMs were imparted to the samples using a 100 mT peak AF, and a 0.05 mT direct current (DC) field and then progressively AF demagnetized up to 70 mT at 10 mT steps. IRMs were imparted at 950 mT. Both ARM and IRM were measured before and after progressive AF demagnetization at 30 mT. In addition, a backfield IRM was measured by first imparting a 950 mT IRM,

rotating the sample 180° and then imparting an IRM at 100 and 300 mT, with remanence measurement made following each step.

The NRM, ARM, and IRM measurements were conducted at the paleomagnetism laboratory at University of Florida. A loop susceptibility meter with a 2 cm × 2 cm opening was used to measure susceptibility along the U-channel samples. All remanence and susceptibility measurements were made every 1-cm along the U-channel samples. Other susceptibility measurements were made with a point susceptibility meter maintained at the Antarctic Research Facility. Hysteresis measurements were conducted at the Institute of Rock Magnetism at the University of Minnesota.

To determine the mean direction from a discrete sample or a measured interval along a U-channel, we use principal component analysis (PCA) (Kirschvink, 1980). For the PCA direction, we find the best-fit line that passes through the vector demagnetization data without any constraint that the line be anchored to the origin of vector demagnetization space. To avoid data possibly contaminated by low coercivity overprints, we do not use demagnetization steps <20 mT in the PCA. The maximum angular deviation (MAD) obtained from PCA provides a measure of how well the observations fit a line. Values less than 10° are typically considered to provide lines that fit the observations well.

Magnetic polarity stratigraphy is based on the paleomagnetic direction and biostratigraphic data. Because the cores are azimuthally unoriented, we mainly use the paleomagnetic inclination to infer polarity (negative inclinations for normal polarity and positive for reversed), though relative changes in declination can be useful.

4.3. Ice rafted debris (IRD) and clast counts

Six cores (cores ELT37-07, DF79-01, DF79-02, DF79-15, DF79-19, and DF79-56), were analyzed for IRD or lonestone counts in 1-cm intervals (Table 1). Counts were based on new X-ray radiographs made from the archive halves of the cores. Only clasts over 1 cm in longest apparent diameter, with well-defined edges, were counted, thereby avoiding the occasional ghost images

produced by X-ray instruments. Additionally, the above new X-ray radiographs and existing X-ray radiographs, from USGS Cores A1G1, A2G2, A8G1, A9G1, and A10G1, were used for textural descriptions.

4.4. Biogenic opal

Percent biogenic opal was determined using the method of Mortlock and Froelich (1989). Biogenic opal is useful (a) as a paleoproductivity indicator because it represents the preserved flux of diatom valves to the seabed, and (b) for correlation with and calibration of the magnetic signal downcore because diatom production in combination with a relatively small input of terrestrial sediment results in a large dynamic range in opal content in Southern Ocean sediment and is often the most important parameter influencing magnetic susceptibility in fine-grained sediment.

5. Age, nature and distribution of sediment on the Wilkes Land margin

5.1. Continental shelf

5.1.1. Inner-shelf basins

Deep (>1000 m water depth) inner-shelf basins are located at the mouth of outlet glaciers along the Adélie and George V Coasts of the Wilkes Land margin (Fig. 2). Initial description of the sediment and fauna recovered from gravity and piston cores raised from these basins during the Deep Freeze 79 and USGS 1984 cruises, were given by Domack (1982), Anderson et al. (1983), Dunbar et al. (1985) and Hampton et al. (1987b). These studies reported that sediment from the inner-shelf basins are characterized by diatomaceous ooze with high (>30%) biogenic silica content.

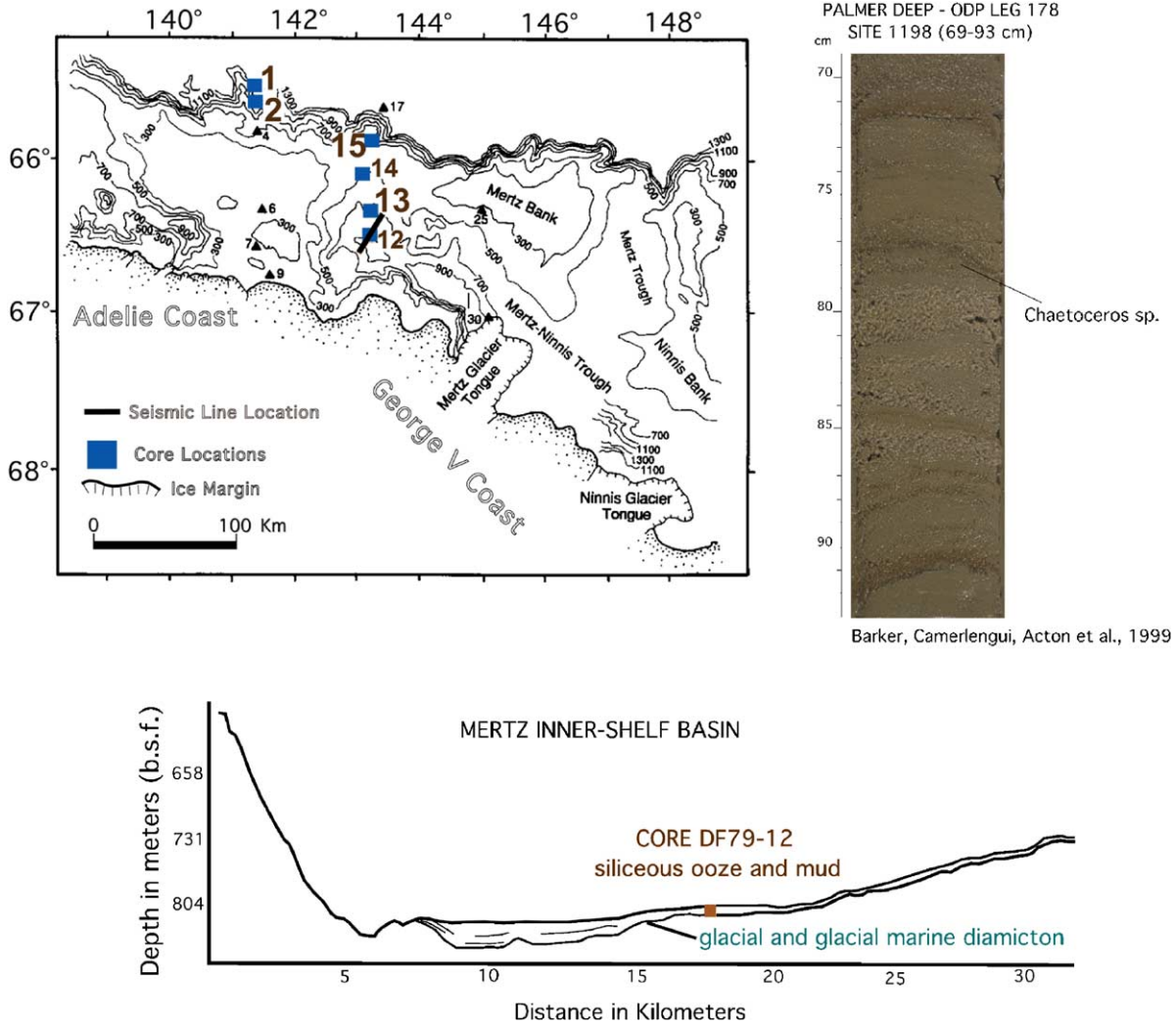
For our study, we conducted detailed diatom analyses on core DF79-13 (Table 2), which sampled the inner-shelf basin located west of the mouth of the Mertz-Ninnis Glacier (Figs. 1–3). Core DF79-13 was collected from 682 m water depth and is 595 cm long. It consists of laminated to stratified diatomaceous mud with abundant “diatom cotton” bloom laminations, and intervals

of high-porosity coincident with diatom-rich intervals, which are similar to sediment recovered from the Palmer Deep, an inner-shelf basin off the Antarctic Peninsula that was drilled during ODP Leg 178 (Fig. 3). New biostratigraphic markers for the Southern Ocean (Zielinski and Gersonde, 2002) such as *R. leventerae* (Last Occurrence Datum, LOD, at 0.13 Ma) and *Rouxia constricta* (LOD at 0.28 Ma) were not registered. Micro-paleontological analysis based on diatom abundances of *Eucampia antarctica* have shown that the latter is rare in Holocene sediment but increases notably during the Last Glacial Maximum (LGM) (Burckle and Cooke, 1983). Core DF79-13 does not show this increase (Table 2, Fig. 4), indicating the approximate age to be younger than 18 Ka. Moreover, our quantitative diatom analyses show that the diatom species present in the core are indicative of fluctuating sea-ice conditions (Fig. 4), with maximum sea-ice conditions recorded at the core top, at 150–210 cm, and at 400 cm. Similar fluctuations, with periodicity of 200–250 years, have been observed on the Bransfield Strait (Leventer et al., 1996; Barcena et al., 1998, 2002). The species considered as sea-ice markers are *Fragilariopsis curta*, *F. cylindrus*, *F. obliquecostata*, *F. ritscheri*, *F. sublinearis* and *F. vanheurckii*.

5.1.2. Shelf troughs

As described by previous workers, sediment cores collected from shelf troughs contain Holocene diatomaceous mud overlying Pleistocene diamicton (Domack, 1982; Domack and Anderson, 1983; Dunbar et al., 1985; Hampton et al., 1987b). For this study we have analyzed in more detail two cores: (1) USGS Core A1G1 collected from the Mertz Trough (Hampton et al., 1987b) at 611 m water depth, and (2) Core DF79-15 collected from the shelf trough located west of the Mertz Glacier (Domack, 1982) at 412 m water depth (Figs. 1, 2 and 5).

Core A1G1 consists of 77 cm of diatomaceous mud overlying 208 cm of massive to crudely stratified muddy diamicton (Fig. 5). The 0–77 cm sediment interval contains abundant open-ocean diatoms typical of the Southern Ocean and is likely Holocene in age. Sediment from ~77 to 265 cm contains mostly fragmented and reworked, largely



Barker, Camerlengui, Acton et al., 1999

Fig. 3. Location of Cores DF79-12 and DF79-13 near the edge of the Mertz-Ninnis inner-shelf basin. Both cores recovered diatomaceous ooze with a high-resolution record of paleoproductivity. The line drawing from a 12 kHz subbottom profiler record from Domack and Anderson (1983), shows a SW-NE cross section of this inner-shelf basin and the location of Core DF79-12. A digital image of Cores DF79-12 and -13 is not available because they were heavily sampled on both the working and archive halves of the cores. However, sediments in the DF79 cores closely resemble the diatomaceous oozes recovered during ODP Leg 178 Site 1098 from the Palmer Deep, a deep inner-shelf basin off the Antarctic Peninsula, which also contains a Holocene high-resolution record. Bathymetry from Chase et al. (1987).

Neogene, diatoms, but a few Pliocene/Pleistocene diatoms are also present. We interpret the intervals containing open-ocean diatoms as interglacial whereas the diamiction containing only a few fragmented diatoms is considered to be glacial. Six paleomagnetic samples collected from 11, 37, 67, 119, 161, and 205 cm have a median NRM

intensity of 4.3×10^{-3} A/m and are all normal polarity (Fig. 6). Though the sampling interval is relatively crude and the potential for hiatuses exist, it is likely that the sampled interval falls within the Chron C1n (the Brunhes normal polarity epoch) and thus has an age less than 0.78 Ma. This age assignment is consistent with the diatom

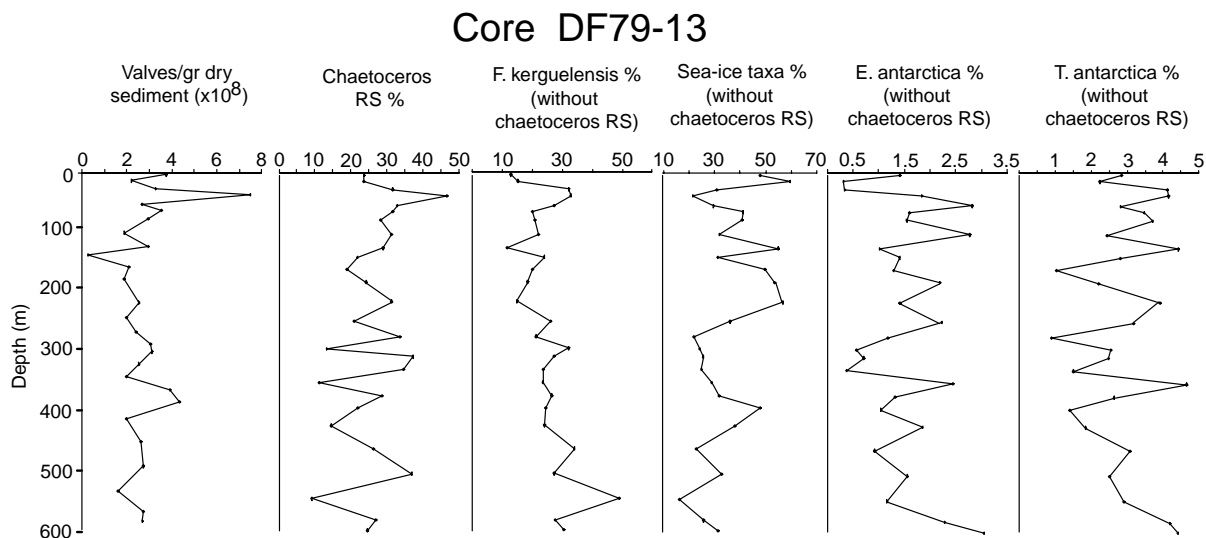


Fig. 4. Plot showing the abundance of diatom species present in Core DF79-13. These species are good indicators of sea-ice conditions during the Holocene with maximum sea-ice conditions recorded at 150–210 and 400 cm.

biostratigraphy given the occurrence of reworked Pleistocene diatoms down to the base of the cored interval.

Core DF79-15 lacks the diatomaceous mud cover that characterizes other cores collected from the shelf trough environment and consists of 360 cm of massive muddy diamicton texturally similar to the diamicton in Core A1G1 (Fig. 5). X-ray radiographs show this diamicton to be clast-supported with abundant (Fig. 7) angular to surrounded pebbles. Core DF79-15 is also similar to A1G1 in diatom abundance and preservation (Fig. 7). Although no stratigraphic marker species (*Actinocyclus inges*, *R. constricta*, *R. leventerae* or *E. antarctica* maximum) were found, the core is probably Pleistocene younger than 0.13 Ma, and the top is older than Holocene. When *Chaetoceros* resting spores and sea-ice species are very abundant, East Antarctica does not have the 18 downcore pattern as described for more open ocean environments (Burckle and Cooke, 1983). The downcore diatom record here could argue for a core top from MIS2 (around 20 kyr BP) and a bottom from the Stage 4/3 transition (around 59 kyr BP). Diatom abundance is two orders of magnitude lower than in core DF79-13, which is deeper in the Mertz Trough than DF79-15, and

the sediment contains a high degree of diatom fragments, but also contains sea-ice taxa as well as open-ocean diatoms reflecting glacial/interglacial intervals (Table 2, Fig. 7).

5.1.3. Shelf banks

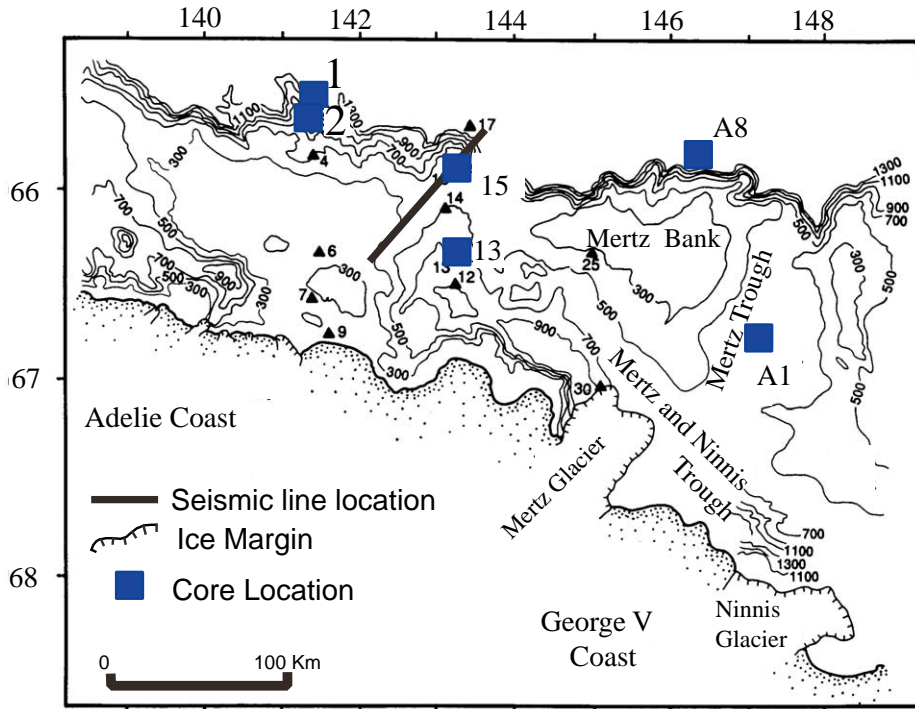
Previous studies reported that continental shelf-bank sediment consists of residual glacial-marine sand and muddy sand with varying concentrations of fine-grained matrix (Domack, 1982; Dunbar et al., 1985; Hampton et al., 1987b). For this study we analyzed USGS Core A2G2 collected near the shelf break on the Mertz Bank at 458 m water depth (Figs. 1 and 2).

Core A2G2 is 139 cm long and consists of massive sandy mud with numerous granules and pebbles scattered throughout. Although diatoms are common in this core, they are mostly fragmented. They consist of a mixture of early Pleistocene and Neogene species, tentatively suggesting an early Pleistocene age for this core.

Other cores not analyzed but examined for this study from the shelf bank environment are characterized either by unsorted sand such as Core DF79-07, or by one or several sequences of graded coarse sand, for example Core DF79-04 (Fig. 8).

USGS A1G1

111 cm



156 cm

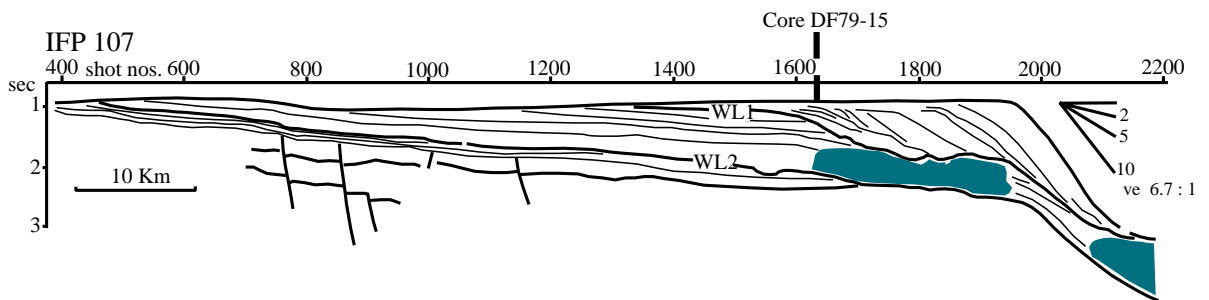


Fig. 5. Textural character of the diamicton recovered in USGS Core A1G1. Also shown is a line drawing of a multichannel seismic line across a shelf trough with the location of Core DF79-15, which has similar textural character than Core A1G1. Note that the resolution of the seismic line is well below the resolution of the sediment cores, and thus no direct correlations can be made.

5.2. Continental slope

According to previous descriptions, sediment cores from the continental slope consist of mud,

silty mud, muddy sands, gravely muddy sand and gravely sandy mud (Payne and Conolly, 1972; Domack et al., 1982; Milam and Anderson, 1981; Anderson et al., 1983; Hampton et al., 1987b). For

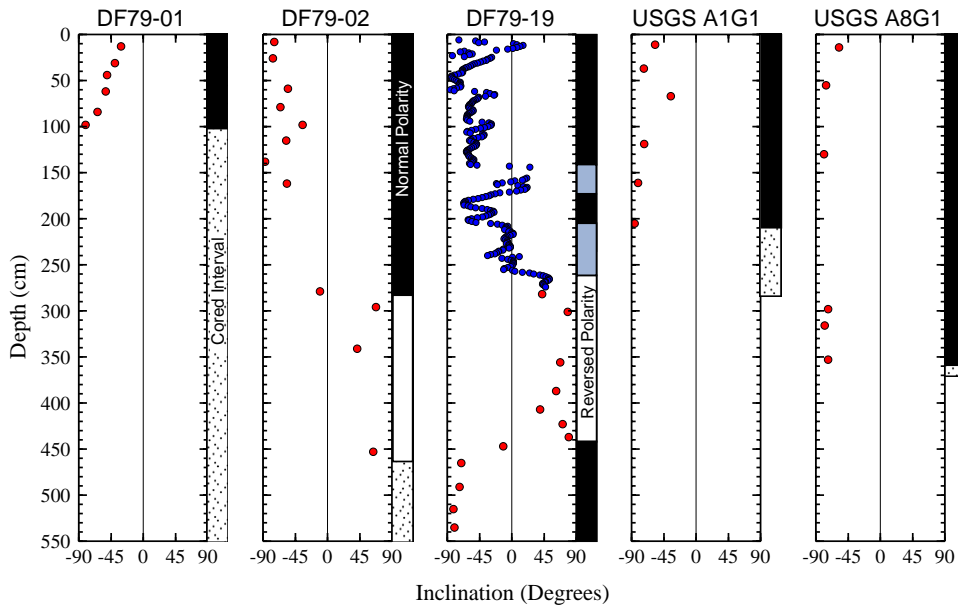


Fig. 6. The magnetostatigraphy of Cores DF79-01, DF79-02, DF79-19, A1G1, and A8G1 are shown with the inclination data from U-channel samples and discrete samples. The mean inclination shown is estimated from principal component analysis. Normal polarity intervals are shown with black boxes, reversed polarity intervals with white boxes, and intervals of uncertain polarity with gray boxes. Intervals cored but not sampled for magnetic measurements are dotted.

our study we analyzed in more detail Core DF79-02 collected from the continental slope at 1098 m water depth (Figs. 1, 2, 8, 9 and 10).

Core DF79-02 is 575 cm long and consists of massive sandy mud to fine sand intervals alternating with massive sandy and pebbly intervals. Clast counts show more abundant clasts than observed in cores further down the slope (Fig. 9). Two main peaks are observed in the cored intervals between ~ 182 – 223 and ~ 277 – 342 cm. On X-ray radiographs, the intervals with more abundance of clasts coincide with massive intervals consisting of fine-grained matrix with clasts, whose texture is similar in appearance to the diamicton recovered from the continental-shelf troughs.

The 13 discrete paleomagnetic samples from this core have a median NRM intensity of 7.0×10^{-4} A/m. Samples from above a gravelly interval (182–233 cm) have normal polarity (Fig. 6). Samples below 233 cm give relatively noisy results, likely caused by coarser-grained lithologies in which the magnetic carrier is more likely to be a multidomain magnetite. At least two of the samples, at 279 and 341 cm, have low negative

inclinations, indicating that at least part of the section has reversed polarity (Fig. 6). The lowest sample, at 453 cm, is reversed polarity. An unambiguous correlation of the polarity intervals with chrons is not possible given the lack of biostratigraphic constraints and the coarse nature of the sediment. The existence of multiple polarities would, however, indicate that the base of the sediment cored is older than the top of Chron 1r.1n (0.99–1.07 Ma).

Biogenic opal analyses on samples from Core DF79-02 show generally low values between 2.69 and 10.46% (Table 3). From the top of the core to a sample at 177 cm the biogenic opal values are $< 5\%$. Below a sample at 233 cm the biogenic opal values are $> 7\%$, increasing down core to 10.46% at the base.

5.3. Base of the slope and upper continental rise

Base of the slope and upper continental rise cores have been described previously as being silty, sandy and pebbly in nature (Payne and Conolly, 1972; Hampton et al., 1987b). For our study, we

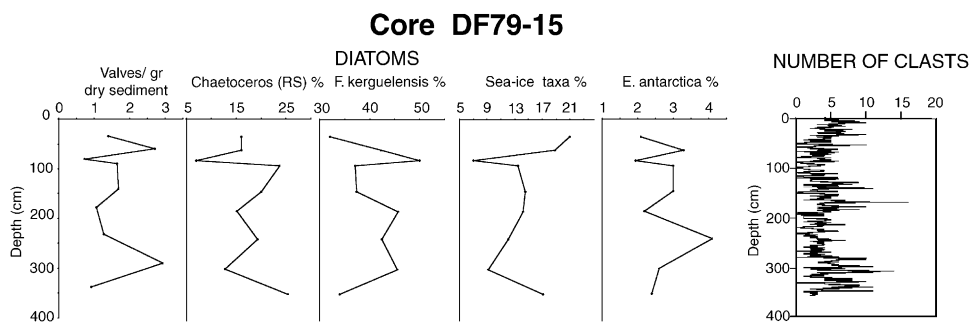


Fig. 7. Plot showing the abundance of diatom species in Core DF79-15. Although the abundance compared with Core DF79-13 has decreased notably, the diatom species present are good indicators of sea-ice conditions. Also shown is the abundance of clasts determined using X-ray radiographs.

analyzed in more detail Core DF79-01 collected from the base of the slope at 2022 m water depth (Figs. 1, 2, 8, 9 and 10), and Cores DF79-56 and DF79-19 collected from the upper continental rise at 2361 m and 2598 m water depth, respectively (Fig. 2).

Core DF79-01 is 555 cm long and consists of mud and silty/sandy mud. In X-ray radiographs we observe massive intervals alternating with either crudely stratified or crudely laminated intervals. Clast counts in this core show few clasts scattered throughout the core with peaks in abundance at 67, 125–130, 160–178 cm, and through the 205–240 interval (Fig. 9). Peaks in abundance of clasts are generally within the massive intervals of the core. The six discrete paleomagnetic samples collected from this core have a median NRM intensity of 1.4×10^{-2} A/m, the highest of all the cores sampled. Samples were only taken from the upper meter of the cored interval. All six samples gave stable univectorial directions, with MAD values $< 5^\circ$ for five samples and inclinations ranging from -31° to -81° (Fig. 6). Thus all samples are normal polarity, indicating that the upper meter of Core DF79-01 most likely was deposited during Chron C1n (0.0–0.78 Ma). Biogenic opal analyses on samples from this core show low values that range between 2.79% and 4.49% (Table 3).

Core DF79-56 is 255 cm long. The top 13 cm consists of non-stratified pebbly sand (fine to coarse) and muddy pebbly sand. The abundance of clasts in the upper 13 cm of the core is shown by quantitative clast counts (Fig. 9). Below 13 cm

there is a sharp decrease in the abundance of clasts scattered throughout the core (Fig. 9). The dominant lithologies from 13 to 255 are silty and sandy mud with sand content decreasing down-core.

Core DF79-19 is 586 cm long and consists of mud, silty and sandy mud, and sand. X-ray radiographs reveal a textural pattern similar to Core DF79-01, with massive intervals alternating with either crudely laminated or finely laminated intervals. Clast counts in this core show a similar pattern to Core DF79-56, with a peak in abundance from 10 to 20 cm and at 50 cm and low abundance clast scattered throughout the rest of the core (Fig. 11). Fig. 11 also shows next to the clast count of this core the associated magnetic susceptibility. It is clear from this figure that neither susceptibility as measured by loop meter or measured by point meter, can be interpreted as a simple proxy for the presence of clasts. Of interest are a few Miocene intervals that contain no clasts whatsoever, similar to results obtained at ODP Site 188–1165 in Prydz Bay (O'Brien et al., 2001). In contrast, all Pliocene samples contain IRD, similar to results obtained at ODP Sites 114–699 and 701 in the subantarctic South Atlantic (Kennett and Hodell, 1993; Warnke et al., 1992) and Site 188–1165 in Prydz Bay (O'Brien et al., 2001).

The top of Core DF79-19 contains mostly fragmented diatoms, but a few Pleistocene diatoms are present (fragments of *A. ingens*, *T. lentiginosa*, *F. kerguelensis*) (Fig. 12). A sample from 51 cm, with high amount of fragmented diatoms, has taxa

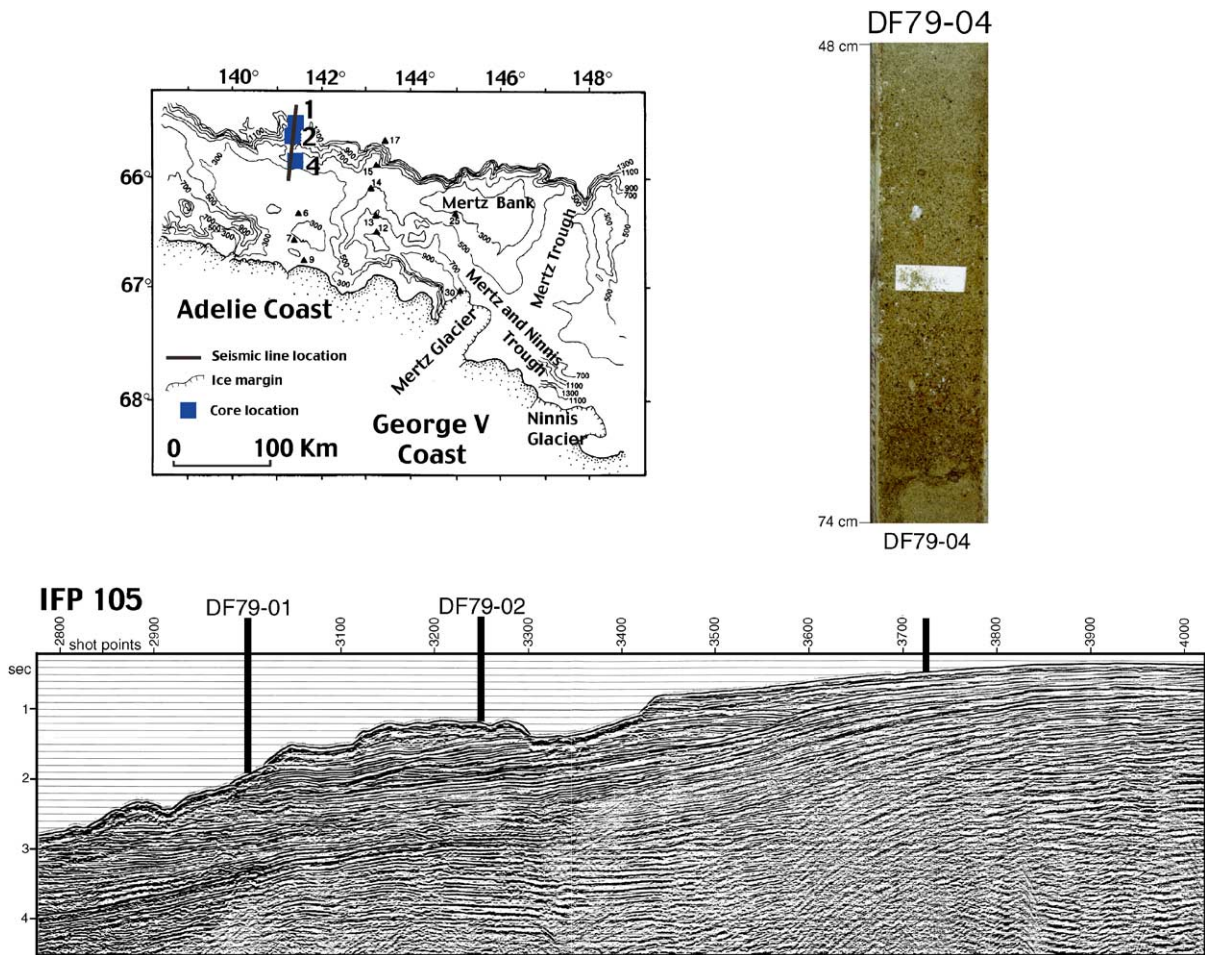


Fig. 8. Textural character of Core DF79-04 from one of the Wilkes Land shelf banks, showing one of the fining-upward sandy intervals observed in this core. Also shown is a multichannel seismic profile across the continental shelf and slope with the location of a transect of three cores: Core DF79-04 from the outer shelf bank and Cores DF79-02 and -01 from the slope. Note that the resolution of the seismic line is well below the resolution of the sediment cores and thus no direct correlations can be made. Bathymetry from Chase et al. (1987).

indicative of a Pliocene age (*F. weaveri* and *A. karstenii*), but also some reworked Miocene taxa such as *D. simonsenii* was observed. The interval between 328 and 144 cm, as well as samples 407 and 460 cm are very poor in whole diatoms but contain taxa from the upper Miocene. From the base to 144 cm, the diatom assemblage, with taxa such as *A. ingens*, *A. karstenii*, *D. simonsenii*, *D. dimorpha*, *D. crassa*, *D. ovata*, *F. aurica*, *F. praecurta* and *P. barboi*, indicates that this section is within *A. kennetii*/*F. praecurta* Zone (after Censarek and Gersonde, 2002).

Paleomagnetic and rock magnetic measurements from 14 discrete samples and 268 intervals along U-channels provide an opportunity to assess Core DF79-19 in greater detail than the other cores. The median NRM intensity is 7.6×10^{-3} A/m. MAD values are less than 10° for 12 of 14 discrete samples and for 253 of 268 measured intervals along U-channel samples, indicating that the sediment has recorded stable directions with few exceptions. Hysteresis parameters from seven discrete samples indicates that the main magnetic carrier is pseudosingle-domain (PSD) magnetite

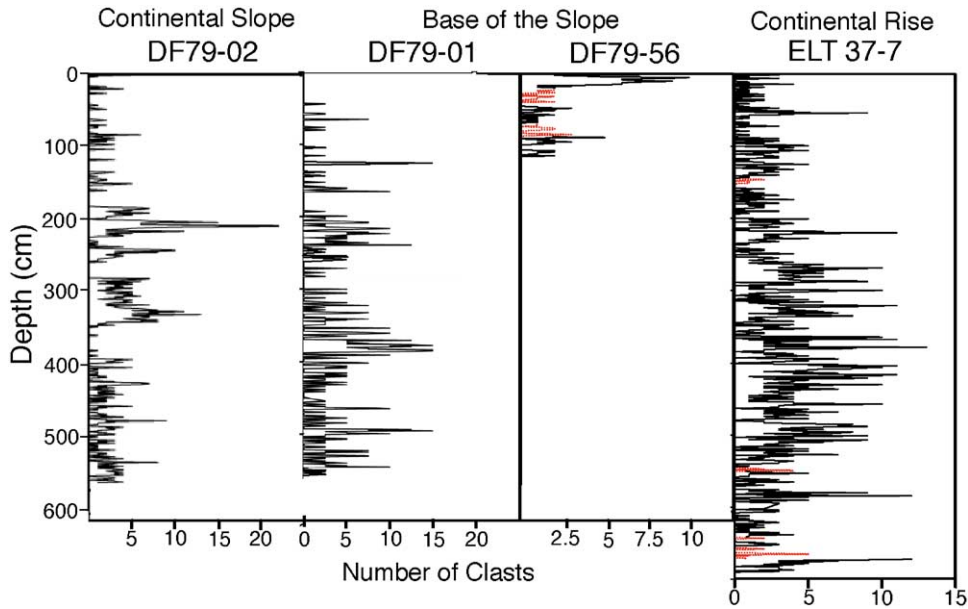


Fig. 9. Textural character of Cores DF79-02 and DF79-01 collected from the continental slope and base of slope respectively. Core DF79-02 is massive with coarser grained intervals similar to the diamicton from the continental shelf. Downslope Core DF79-01 has some stratification and even some crude laminations.

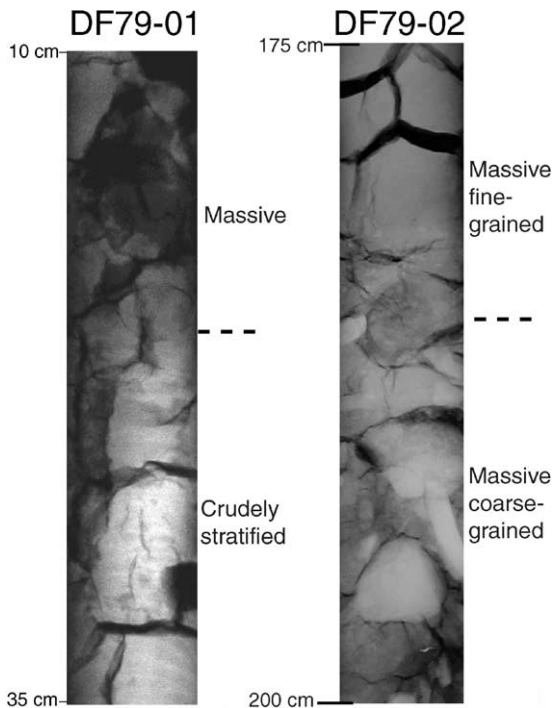


Fig. 10. Clast abundance plots in a core transect from the continental slope to the rise.

(Fig. 13), though we suspect multidomain (MD) grain sizes are present in the regions with high IRD as was observed off the West Antarctic Peninsula by Guyodo et al. (2001). An indication of where MD grain sizes exist can be ascertained from the rate at which the ARM and IRM decay upon AF demagnetization. For large MD grains of magnetite, the IRM is more resistant to AF demagnetization than ARM, whereas the opposite is true for smaller grain sizes (Lowrie and Fuller, 1971). With the exception of short intervals at 45–60, 130–135, 165–167, and 193–198 cm, the IRM decays more rapidly than the ARM, which is consistent with PSD grain sizes. Three of the four short intervals where the ARM decays more rapidly than the IRM are associated with peaks in IRD, where large grain sizes would be expected.

The magnetic polarity for Core DF79-19 consists of at least one normal polarity interval above about 240 cm depth and at least one normal polarity interval below 447 cm depth, with a reversed polarity interval in between (Figs. 6 and 11). Within the interval from 0 to 240 cm that is dominantly normal polarity, two short zones with

Table 3

Percentage opal in samples from cores DF79-01, DF79-02 and ELT37-7. Duplicate analyses were run on each sample and the % error column is the pipetting precision between the two

Core	Sample depth (cm)	Si (%)	SiO ₂ (%)	Opal (%)	Error (%)
DF79-01	0.5	1.33	2.85	3.20	0.01
	30	1.44	3.09	3.46	0.00
	60	1.38	2.95	3.31	0.00
	90	1.71	3.66	4.11	0.00
	120	1.16	2.49	2.79	0.00
	150	1.87	4.01	4.49	0.01
	180	1.51	3.24	3.63	0.00
	210	1.69	3.61	4.05	0.01
	244	1.49	3.18	3.57	0.00
	262	1.51	3.24	3.63	0.00
	278	1.8	3.85	4.32	0.01
	289	1.63	3.49	3.92	0.00
	304	1.79	3.82	4.29	0.00
	324	1.48	3.16	3.54	0.00
	346	1.32	2.82	3.16	0.02
	374	1.4	3.00	3.36	0.01
	384	1.49	3.19	3.58	0.01
414	1.65	3.54	3.97	0.00	
522	1.53	3.27	3.67	0.01	
DF79-02	0	1.12	2.40	2.70	0.01
	8	1.58	3.37	3.78	0.01
	26	1.22	2.60	2.92	0.00
	46	1.82	3.89	4.36	0.00
	59	2.05	4.38	4.91	0.01
	79	2	4.27	4.80	0.01
	94	1.46	3.13	3.51	0.00
	98	1.49	3.19	3.58	0.00
	115	1.12	2.40	2.69	0.00
	127	1.44	3.08	3.46	0.01
	138	1.85	3.97	4.45	0.01
	152	1.66	3.54	3.97	0.00
	162	1.45	3.09	3.47	0.00
	177	1.69	3.62	4.06	0.00
	233	3.02	6.47	7.26	0.03
	260	3.12	6.67	7.48	0.01
	279	3.12	6.67	7.48	0.01
296	3.04	6.51	7.30	0.00	
ELT37-7	0	2.67	5.70	6.40	0.02
	15	2.07	4.43	4.97	0.01
	46	2.32	4.97	5.58	0.01
	75	1.99	4.27	4.79	0.00
	93	2.18	4.67	5.24	0.01
	115	1.94	4.15	4.66	0.00
	131	2.02	4.32	4.85	0.00
	150	1.72	3.69	4.14	0.00
	179	2	4.28	4.80	0.00
	204	2.1	4.49	5.03	0.02
	224	2.34	5.01	5.62	0.00

Table 3 (continued)

Core	Sample depth (cm)	Si (%)	SiO ₂ (%)	Opal (%)	Error (%)
	270	3.36	7.18	8.05	0.01
	295	2.38	5.10	5.72	0.00
	310	1.76	3.76	4.22	0.01
	335	2.85	6.10	6.84	0.02
	366	2.5	5.35	6.00	0.01
	408	2.38	5.08	5.70	0.02
	445	2.98	6.38	7.16	0.01
	478	3.28	7.02	7.88	0.01
	514	6.21	13.28	14.90	0.02
	553	3.69	7.89	8.85	0.02
	584	5.59	11.95	13.41	0.01
	594	4.69	10.02	11.25	0.00
	606	6.62	14.16	15.89	0.02
	628	2.07	4.42	4.96	0.01
	648	2.9	6.21	6.97	0.00
	667	1.78	3.81	4.27	0.01
	687	2.18	4.67	5.24	0.02
	713	2.79	5.97	6.70	0.00
	736	3.15	6.73	7.55	0.01
	766	4.77	10.20	11.44	0.01
	795	3.26	6.97	7.82	0.00
	816	5.28	11.30	12.68	0.01

shallow positive inclinations occur at depths of 10–15 cm and 144–170 cm (Fig. 11). The upper zone is within an interval of high IRD and the lower zone has low intensity and shows little change in declination relative to the normal polarity zones above and below it. Thus, we do not consider either of these to be reversed polarity zones, rather they are artifacts of deposition, coring, or measurement or are possibly excursions. Given that the biostratigraphic constraints indicate that recent sediment is missing from the section and that the mean age of most of the section is likely between about 2–10 Ma, the normal–reversed–normal polarity sequence most likely corresponds with chrons between Chron C2n and C5n.2n (Fig. 11). A unique correlation with chrons of the geomagnetic polarity timescale is not possible without tighter independent age constraints.

5.4. Continental rise

As reported in previous studies, continental rise sedimentation is characterized by massive mud

and laminated sand and mud (Payne and Conolly, 1972; Hampton et al., 1987b). For our study, we have analyzed in more detail USGS Cores A8G1, A9G1 and A10G1 collected from 2635, 3037, and 3379 m water depth, respectively, and Eltanin Core ELT37-07 collected from 3186 m water depth (Figs. 1 and 2).

Cores A8G1 and A9G1 are 369 and 368 cm long, respectively, and consist of massive mud to sandy mud alternating with laminated mud as previously described by Hampton et al. (1987b) and as shown in Fig. 14. The fine laminae on this core were previously interpreted as the result of deposition by bottom contour-currents (Hampton et al., 1987b; Escutia et al., 2002). Samples from the top of Core A8G1 to 131 cm contain abundant diatoms indicative of Pleistocene age, likely younger than isotopic Stage 7, and of an open-ocean environment. Samples collected from Core A8G1 from 213 to 353 cm contain common to few diatoms, mostly fragmented. These diatoms are of Pliocene/Pleistocene age with reworked Neogene forms. The six paleomagnetic samples from Core A8G1 are normal polarity (Fig. 6), consistent with the entire cored section being deposited during Chron C1n (0.0–0.78 Ma). Samples from Core A9G1 at 15, 218, 244, and 313 cm contain abundant diatoms indicating a Pleistocene, likely younger than isotopic Stage 7 based on the absence of *Hemidiscus karstenii*, and an open-ocean environment of deposition. Samples from Core A9G1 at 75 and 155 cm contain few fragmented diatoms of Pleistocene age.

Core A10G1 is 375 cm long and consists of massive mud to silty mud alternating with laminated silty to sandy mud as described previously by Hampton et al. (1987b) and as illustrated in Fig. 15. Samples from 10 to 12, 38, 244, and 313 cm have abundant Pleistocene diatoms, likely younger than isotopic Stage 7 based on the absence of *Hemidiscus karstenii*, indicative of an open-ocean depositional environment. Samples from 68 and 244 cm are similar to the sample from 38 cm but the diatoms are more fragmented.

In all the continental rise cores described above, the core intervals containing abundant open-ocean diatoms are interpreted to be deposited during an

interglacial period. The core intervals containing mostly fragmented diatoms are considered to be glacial intervals.

Core ELT37-07 is 856 cm long and consists of mud and silty mud becoming muddier below 310 cm. X-ray radiographs show the core to consist of massive intervals (e.g., between 0–132, 158–542, 550–610, 635–640, 647–655 and 672–693), which are interbedded with crudely stratified to laminated intervals. Below 542 cm, massive intervals become thinner with depth (i.e. 60–8 cm thick) and are interbedded with crudely laminated to laminated intervals that are 8–15 cm thick. Clast counts in this core show peaks in abundance of clasts at 48, 220, 260–520, 580, and 672 cm (Fig. 9). The clast peaks are all within the massive intervals in the core. Table 3 shows the biogenic opal content on samples from this core, which is in general low throughout the core. High opal-percentage values correspond with the massive intervals of the core, while lower values correspond with the laminated intervals.

6. Sedimentation rates and hiatuses

Assuming that the surface sediment was recovered and represents present age, minimum sedimentation rates can be established by using diatom biostratigraphy for the bottom samples of the cores analyzed for this study and magnetostratigraphy when available. The 595-cm-thick diatomaceous mud recovered from the inner-shelf basin Core DF79-13 has been dated younger than 18 kyr BP. The LGM extended from 22,000–14,000 BP (Dreimanis and Goldthwait, 1973; Crowley and North, 1977). In Antarctica, a significant sea ice retreat began 15,000 BP (Labreyrie et al., 1986), with surface water temperatures reaching present levels by 13,000 BP (Labracherie et al., 1989). Another last abrupt warming occurred 10,000 BP following the colder Younger Dryas (YD). Taking this information into consideration, minimum sedimentation rates in inner-shelf basins using a time range between 15,000 and 10,000 BP are estimated to be between 39.7 and 59.5 cm/kyr, respectively.

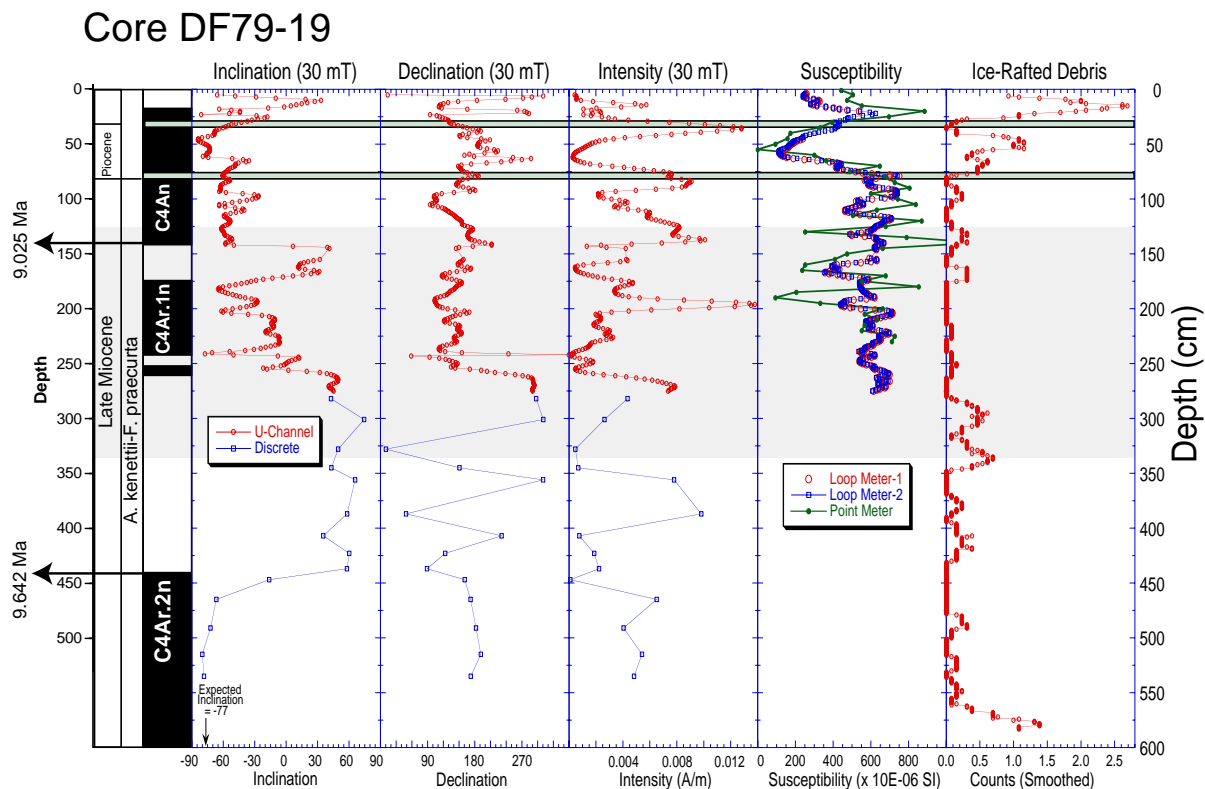


Fig. 11. One possible interpretation of the magnetic polarity stratigraphy for Core DF79-19 based on the biostratigraphic data. Also shown are the paleomagnetic remanence measured on U-channel and discrete samples, the magnetic susceptibility, and clast counts (smoothed over an 11-cm window). The cores are azimuthally oriented so the declination is only relative. The core presents frequent hiatuses as observed from the diatom stratigraphy.

Minimum sedimentation rates for the shelf trough environment are calculated using diatom stratigraphy from Cores A1G1 and DF79-15. In our calculations we assume that no hiatuses exist within the recovered interval. However, seismic profiles from shelf trough environments record numerous erosional surfaces produced by grounded-ice advance during glacials, and thus hiatuses are possibly present in the cores. The presence of hiatuses is further supported by the fact that the Holocene section is not recovered in all the cores collected from the continental-shelf trough environment. With all the above in mind, sedimentation rates for the upper 77 cm of diatomaceous mud recovered and dated Holocene are between 5.6 and 7.7 cm/kyr. The lower 188 cm of Core A1G1 consists of Pleistocene diamicton. Core DF79-15 consists of 360 cm of diamicton

younger than 130 kyr BP. If as argued earlier we consider an age of around 20 kyr BP for the top of the core and around 59 kyr BP for the bottom, and sedimentation rates for this interval are therefore estimated to be about 9.2 cm/kyr.

Diatom and magnetostratigraphic analyses of sediment from upper-rise Core DF79-19 show the top 35 cm of the core to be of Pleistocene age, younger than 78,000 years BP. Assuming that the top 35 cm of sediment have thus been deposited between 10,000 years (Holocene) and 78,000 years BP, minimum sedimentation rates on the upper continental rise during this period are 0.53 cm/kyr. At 35 and 80 cm, two major hiatuses are indicated by diatom stratigraphy. Below the 35 cm hiatus, the core contains taxa indicative of Pliocene and Miocene age and is normally magnetized. This part of the core is of probable Pliocene age, and

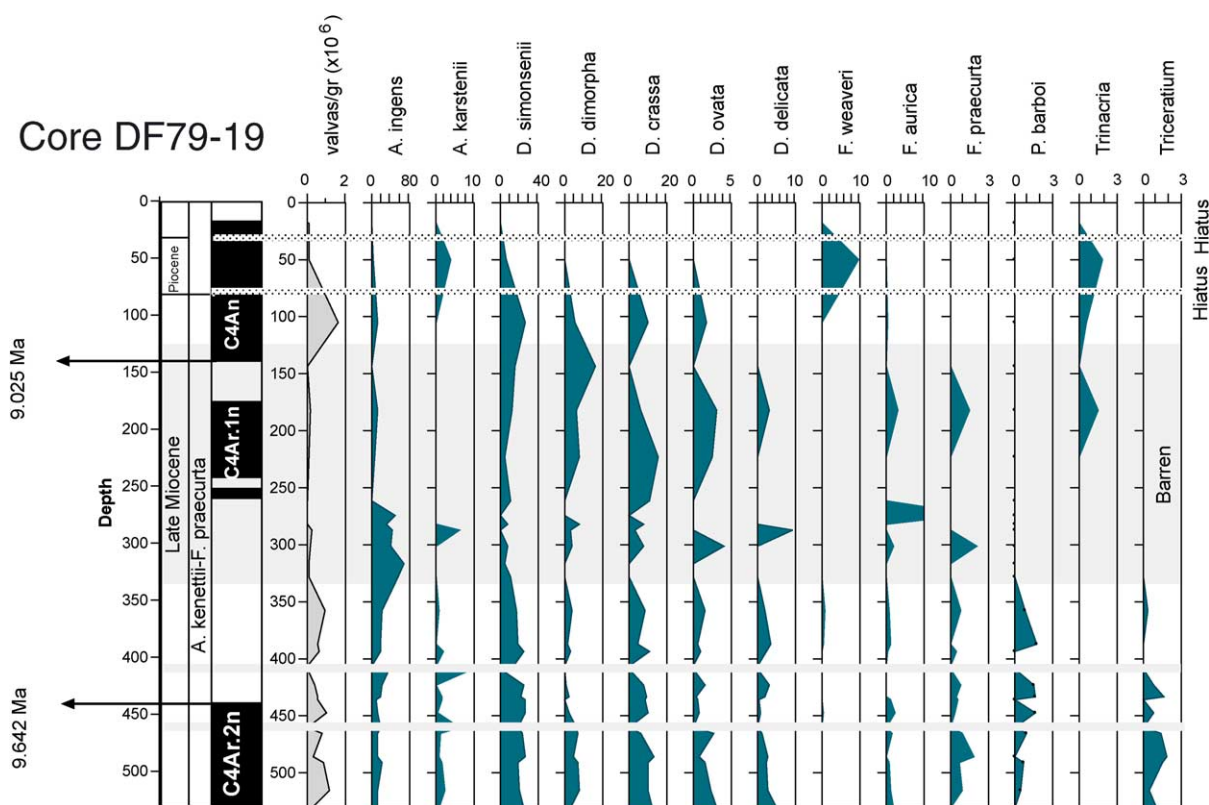


Fig. 12. Diatom stratigraphy from Core DF79-19 collected from the base of the slope. Also shown is the magnetostratigraphy based on the biostratigraphic data. Note that two hiatuses are recognized and that most of the section has an assigned Late Miocene age.

the normal magnetic field interval may represent a condensed Gauss Chron (i.e., 2.60–3.55 Ma). Minimum sedimentation rates for the interval between the two hiatuses is 0.05 cm/kyr. Below 80 cm, the core contains taxa typical of the upper Miocene. Based on our interpretations of diatom and magnetostratigraphic data, minimum sedimentation rates for the entire interval from 80 to 447 cm are 0.06 cm/kyr (or 59 cm/Ma). Fig. 12 shows the bottom of Chron C4An (9.025 Ma) at 140 cm downcore, and the top of Chron C4Ar.2n (9.642 Ma) at 447 cm. Based on this information, the interval from 80 to 140 cm has extremely low minimum sedimentation rates of 0.01 cm/kyr, but the interval from 140 to 447 cm has a sedimentation rate of 0.50 cm/kyr. Our estimates of accumulation rates below the 35 cm interval are not reliable because we do not have good age constraints to know how much of the section is

missing. We expect sedimentation rates to be closer to rates calculated in other Antarctic margins for the same time intervals. For example, Continental rise ODP Sites 1095, 1096 and 1101 drilled during Leg 178 (Barker et al., 1999) gave sedimentation rates of 5–18 cm/kyr for the upper Miocene and 2.5–8 cm/kyr for the lower Pliocene. Sedimentation rates measured at ODP Site 1165 drilled during Leg 188 in Prydz Bay (Shipboard Scientific Party, 2001) decreased from ~1.5 cm/kyr during the upper Miocene to ~0.7 cm/kyr during the upper Pliocene and Pleistocene.

7. Sedimentary processes

Two important factors controlling the type, volume, and distribution of sediment in the Wilkes Land margin during the Cenozoic are the long-

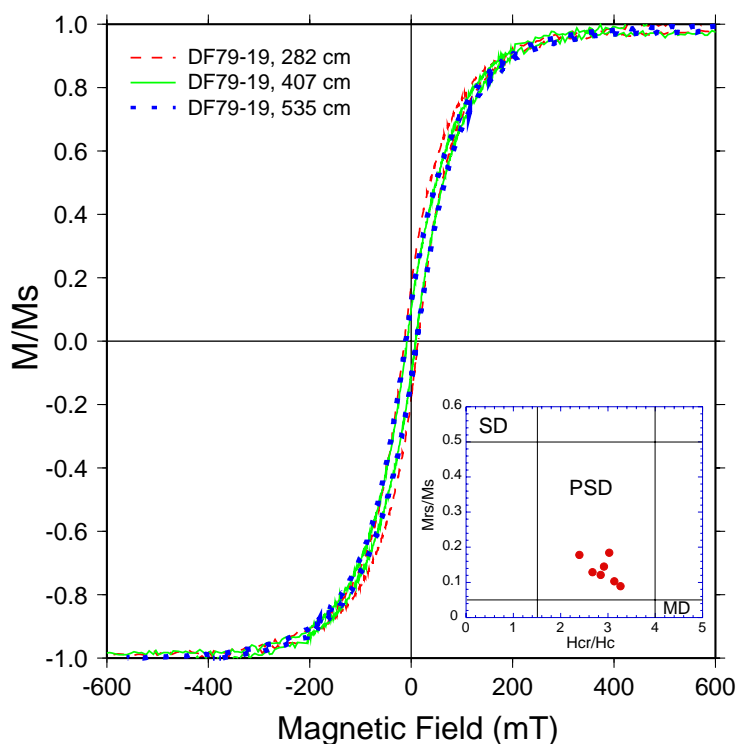


Fig. 13. Three hysteresis loops for samples collected from Core DF79-19. The magnetizations (M) are normalized by their values at saturation magnetization (M_s). The inset shows magnetic grain size distribution, as indicated by variations in the hysteresis parameters (Day et al., 1977), where SD is single domain, MD is multi-domain, and PSD is pseudo-single domain grain sizes.

term variations in the polar regime of the continent, and the glacial–interglacial cycles. During the Quaternary, when polar regime has dominated in the Antarctic continent, glacial and interglacial cycles are one of the main factors determining the sediment type, volume of sediment supply, and what sedimentary processes are active in the margin. The Adelie and George V Coasts of the Wilkes Land margin drain the East Antarctic Ice Sheet with a mostly divergent flow pattern. The present coastline is characterized by ice cliffs and individual outlet glacier systems, such as the Ninnis and the Mertz. These outlet glaciers have an important role in ice drainage and sediment delivery to the ocean (Drewry and Cooper, 1981). Drainage velocities in outlet glaciers range from more than 0.5 km/yr to about 3.7 km/yr (Lindstrom and Tyler, 1984; MacDonald et al., 1989), while drainage in the areas in between them, occupied by sea cliffs, may range from few meters to tens of meters every

year (Anderson, 1999). During Pleistocene glacial periods, outlet glaciers advanced onto the shelf as grounded ice streams eroding the deep (> 1000 m) basins in the inner shelf and the large erosional troughs that extend from the inner-shelf basins to the outer shelf. Between the troughs that are carved by the rapidly moving ice streams, are shallow banks where the ice is implied to have been slow-moving. The present shallow banks on the shelf, however, may not have been permanent features. Buried troughs and prograding wedges, similar to the ones developed in front of the present day outer-shelf troughs, have been described in the Wilkes Land continental shelf underlying some of the more recent flat-lying aggraded sediment of the present banks, based on seismic lines (Fig. 9 in Eittrheim et al., 1995). This suggests that ice streams may have shifted position during consecutive glacial advances (Eittrheim et al., 1995; Escutia et al., 2000).

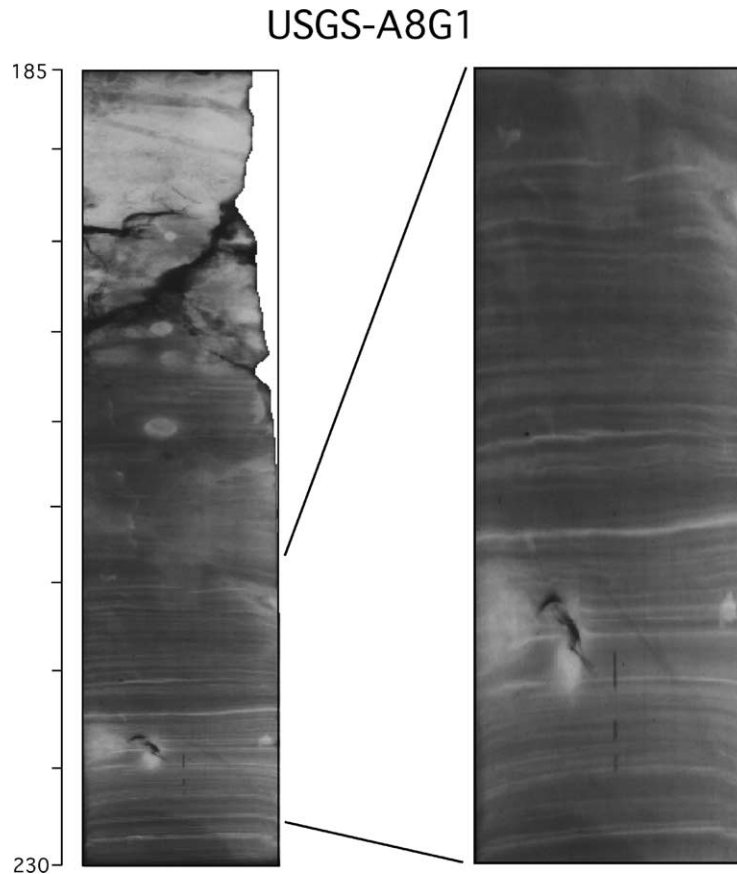


Fig. 14. Textural character of Core A8G1 from the continental rise. Sediment from this environment is characterized by massive bedding, such as shown at the top of the figure, interbedded with laminated intervals. The fine laminae shown in the figure have been interpreted as contourites (Hampton et al., 1987a, b; Escutia et al., 2002).

7.1. Sedimentary processes during the Holocene

The Holocene corresponds with a warm period of time that coincides with glacial continental polar conditions in Antarctica. In the deep (> 1000 m) inner-shelf basins that lie at the mouth of the outlet glaciers, Holocene sedimentary processes are dominated by a rain of the products of biogenic activity as indicated by the diatomaceous ooze and mud in Core DF79-13. This sediment accumulates rapidly during changing sea-ice conditions, with maximum sea-ice conditions recorded at the core top, at 150–210 and 400 cm. Similar fluctuations, with periodicity of 200–250 years, have been observed in the Bransfield Strait (Leventer et al., 1996; Barcena et al.,

1998, 2002), and have been considered as Holocene neoglacial events (Barcena et al., 1998, 2002). The oozes recovered in Core DF79-13 are also similar to those recovered from the Palmer Deep west of the Antarctic Peninsula during ODP Leg 178 (Barker et al., 1999), which also contain a high-resolution record of paleoproductivity that allows further investigation of the global extent of climate events presently defined in regional oceanic data (e.g., Younger Dryas in the North Atlantic) and the evaluation of the potential mechanisms that link biological productivity and climate in the Southern Ocean. Very-high-resolution chirp seismic-reflection data and new cores raised from the Wilkes Land Mertz-Ninnis inner-shelf basin environment during the WEGA-2000

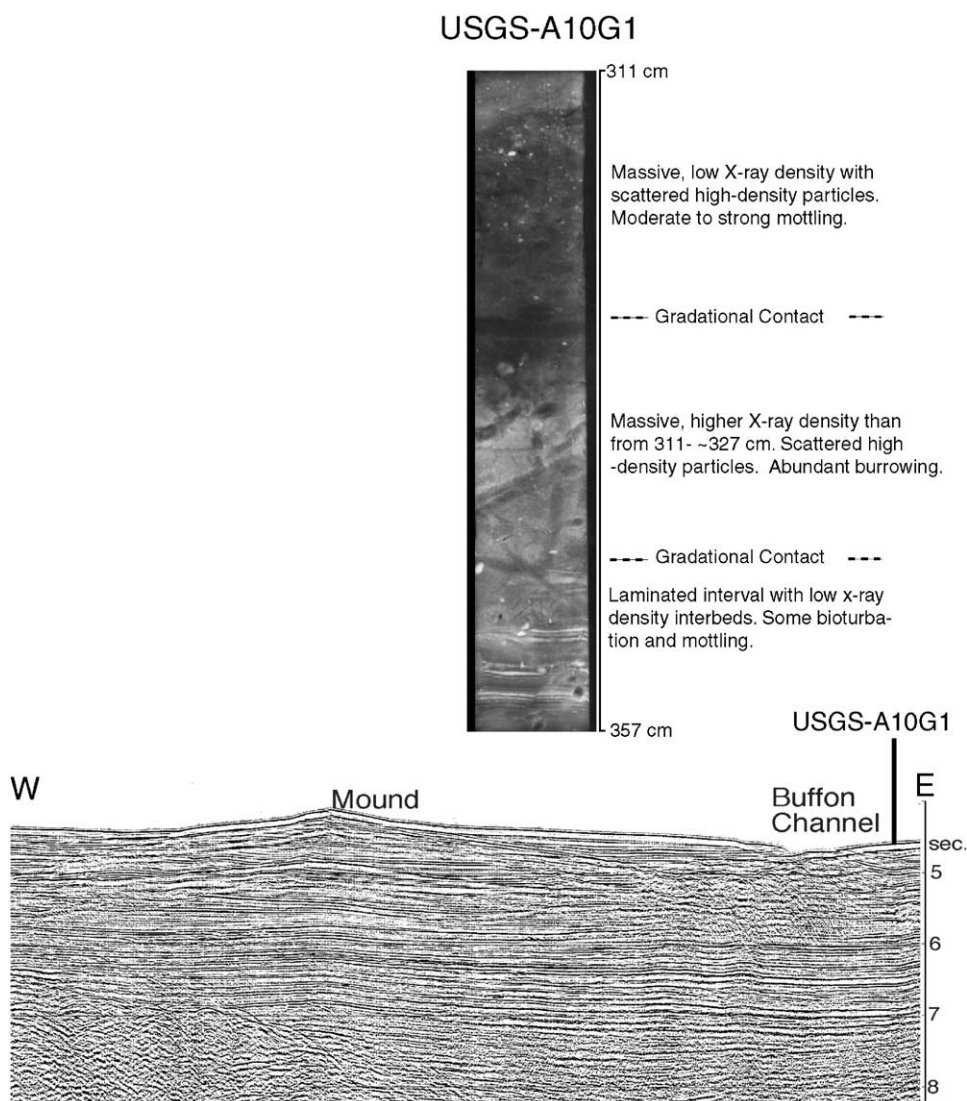


Fig. 15. Textural character of one of the most distal continental rise cores, USGS A10G1, showing the massive bioturbated interglacial intervals alternating with the laminated glacial intervals. Also shown is a multichannel seismic profile showing the provenance of this core in the east overbank of the Buffon Channel.

Italian-Australian cruise reveal that these cores are from a sediment drift now termed the “Mertz Drift” (Presti et al., 2001).

Holocene sedimentation in the shelf troughs that extend seaward from the deep inner-shelf basins, when present, is characterized by diatomaceous mud, which suggests that sedimentation is dominated by settling of fine-grained hemipelagic

sediment with a significant biogenic component. Changes in the thickness of these deposits (from 0 to ~77 cm in the studied cores) are likely to result from the irregular glacial topography of the seafloor and from erosional processes, such as bottom currents or ice keels furrowing the seafloor (Barnes, 1987). Re-sedimentation processes by bottom currents are also suggested by the

well-sorted sand and gravel sediment in shallow banks. Winnowing by bottom-currents on the Wilkes Land shallow banks and the shelf edge (where strong impinging deep-sea currents occur) was already reported by Dunbar et al. (1985), and is a common process on continental shelves around Antarctica (Anderson et al., 1983).

We have not been able to date Holocene sediment on the continental rise. Dates from the top of the cores raised from the base of the slope and rise give Pleistocene ages that are younger than Marine Isotopic Stage 7 (e.g., A8G1). There is the possibility that Holocene sediments are thin and are lost during the coring process.

7.2. *Sedimentary processes during the Pleistocene*

During the Pleistocene glacial, when grounded ice sheets extended on to the Wilkes Land continental shelf, massive to crudely stratified diamicton characterized sedimentation in the Wilkes Land shelf troughs. Based on differences in the texture between these diamictons, Anderson et al. (1980) and Domack (1982) reported that some of the massive diamictons in the Wilkes Land margin included till. Other massive diamicton and crudely stratified diamicton from the Wilkes Land shelf trough environment are interpreted to represent glacial-marine sedimentation in front of the grounding line. This is supported by the geometry of the outermost shelf reflectors imaged in multichannel seismic data (Fig. 5) and high-resolution airgun seismic lines collected across the Wilkes Land shelf troughs. In these profiles, seismic facies are characterized by steep (slopes of about 10°) foresets that fill buried troughs and prograde the outer continental-shelf edge (Fig. 5) (Eittreim and Smith, 1987; Eittreim et al., 1995; Tanahashi et al., 1994; Escutia et al., 1997; Barker et al., 1998). Prograded wedges are common around the Antarctic continental shelf and slope (Larter and Barker, 1989; Bartek et al., 1991; Cooper et al., 1991; Kuvaas and Khristofersen, 1991; Barker et al., 1998) and are particularly well-developed opposite to the main terminations of modern ice-streams. Drilling of prograded wedges around Antarctica has shown that their seismically defined geometry is climate

dependent. Topset seismic facies represent till deposition directly beneath the ice stream (Barker et al., 1999; O'Brien et al., 2001). Foreset seismic facies result from deposition of sediment transported at the base of the ice-stream to the grounding zone. The resulting massive or crudely stratified diamicton has similar characteristics to debris flow deposits.

We are aware that: (1) The sediment recovered by piston coring and analyzed for this study represents strata beyond the resolution of the available seismic lines (Fig. 4). (2) Most of the foreset sequences in Fig. 4 represent strata older than Quaternary. (3) The Quaternary is not entirely representative of glacial sedimentation during earlier times. That said, the fact that during the Pleistocene the ice sheet advanced to the outermost shelf, as reported in: previous studies on sediment cores (Milam and Anderson, 1981; Anderson et al., 1983; Domack et al., 1985; Domack et al., 1989), as evidenced by dating of the shelf cores in this and previous studies (Domack et al., 1989), and as implied by the erosion of all previously deposited and preserved topset strata (Fig. 4), suggests that at least the most recent foreset strata (i.e. foresets in the outermost shelf) are likely representative of processes active during the Quaternary. Debris flows could be generated with minimal triggering on the steep slopes ($\sim 10^\circ$) of this depositional environment. Because earthquakes are not common in this margin, triggering could occur by sediment overloading at the shelf break, which would create instability and generate slumps. Anderson et al. (1979) also suggested that the isostatic rebound that occurs after the ice sheet retrieves from the shelf is an important mechanism for generation of failures, which would generate gravity flows, in the Antarctic continental shelves.

Glacial sediment recovered from shelf banks is characterized by well-sorted and rounded to angular sand and gravel. These deposits can be either graded or non-graded and represent redistribution of the original glacial deposits, likely diamictons. The common absence of mud in these deposits and their well-sorted nature suggest that the finer component of the original deposit was removed and the coarser component sorted as the

different particle sizes settled with varying carrying capacity of the bottom flows. Presence of graded deposits is indicative of gravity flows (i.e. turbidity flows and grain flows) as important process in re-sedimentation of the original glacial deposits. The irregular relief of the Wilkes Land continental shelf provides the necessary slope for initiation of gravity flows. Similar deposits interpreted as gravity flows were collected from the Antarctic Peninsula continental shelf during ODP Leg 178 (Barker et al., 1999).

Slope sedimentation during glacials is characterized by massive sandy mud to fine sand alternating with massive sandy and pebbly deposits (e.g., Core DF79-02), which resemble the diamictos of the continental shelf. Base-of-slope and upper continental rise sedimentation is characterized by overall finer-grained deposits (i.e. mud and silty to sandy mud). These deposits are characterized by alternating massive intervals with abundant IRD, and crudely stratified to laminated intervals with less IRD (e.g., Cores DF79-01 and -19). Diatom analysis on DF79-19 from the upper rise reveals the existence of numerous hiatuses with Quaternary sediment present at the top of the core, with Pliocene sedimentation at 51 cm downcore, and Miocene taxa from 328 cm to the end of the core (Fig. 11). This suggests repeated erosional episodes in this depositional environment. Farther downslope, continental rise sediment consists of mud and silty mud with alternating massive intervals with more abundant IRD, and laminated silty to sandy mud (e.g., Cores A8G1 and A10G1) (Fig. 9). All diatom samples collected from lower rise sediment piston cores that are up to 315 cm long give Pleistocene ages, suggesting a near-continuous mode of sedimentation in the distal rise environment. The transition from an overall coarser-grained and massive sediment on the slope to a finer-grained and laminated sediment on the rise suggests that downslope gravity flow processes were active (if not dominant) during the Pleistocene. Hampton (1972) illustrated how gravity flows transition from slumps to turbidity flows as water is added to the flow. In our case, sediment from slope cores such as Core DF79-02, with a texture that greatly resembles the diamictos on the shelf, would likely represent either part of a

slump block or the proximal part of a debris flow. The crudely stratified to laminated intervals in Core DF79-01 would represent the transition between a debris flow and a turbidity current. Some of the laminated intervals in cores from the continental rise, such as A10G1, probably represent sediment deposited from a turbidity current. The laminated intervals in cores from the continental rise have been previously interpreted as the result of deposition by turbidity currents (Payne and Conolly, 1972; Hayes et al., 1975; Hampton et al., 1987b; Escutia et al., 2002).

Bottom contour-current deposition is also an active process on the continental rise as previously described by Hayes et al. (1975), Hampton et al. (1987b), and Escutia et al. (2000). Escutia et al. (2002) postulate that the suspended fines from the turbidity current flow are entrained in a nepheloid layer associated with westward flowing paleo-bottom currents like those of the AABW that presently sweep the Wilkes Land continental rise below 2500 m water depth. Contourite deposition is evident as laminated silts in cores from the continental rise as for example A8G1 and A10G1 (Figs. 14 and 15). Bottom-contour-current deposition has been a long-lasting process in this margin as evidenced by the sediment mounds that developed in the continental rise interchannel areas, which are well imaged in multichannel seismic profiles (Escutia et al., 1997; Escutia et al., 2000, 2002) (Fig. 15).

During the Pleistocene interglacials, sedimentation was characterized by massive and more IRD-abundant hemipelagic sediment between the glacial stratified to laminated intervals (e.g., Figs. 14 and 15). Based on our limited opal analyses, although the overall biogenic input to the continental slope and rise is generally low, the high opal contents correspond with the massive interglacial intervals (Table 3). Our opal data also show that the biogenic component is more abundant in samples collected from the continental rise (e.g., Core ELT37-07), than in samples from the slope and base of the slope (Cores DF79-02 and -01, respectively) (Table 3). (Also during interglacials, the supply of IRD to the continental rise appears to have been greater relative to the fine-grained terrigenous contribution. During the deposition of

the laminated intervals, IRD contribution was diluted by delivery of fine-grained terrigenous sediment to the rise. The deposition of IRD therefore seems linked to interglacials rather than to periods of glacial maxima. Erosion and re-deposition of fine-grained sediment by bottom countour currents is likely another important process during interglacials. Present-day circulation of the Antarctic Bottom Water (AABW) along the Wilkes Land continental slope and rise is from east to west (Eittrheim et al., 1971). Salinity distribution indicates that dense Ross Sea water spills into the South Indian Basin along the continental margin at about 140°E where it flows westward below 2000 m depth (Eittrheim et al., 1971; Gordon and Tchernia, 1972). The highest velocities (> 15 cm/s) in the South Indian Ocean sector adjacent to the Wilkes Land margin occur in water depths of 684–3440 m. High-velocities and the shear producing irregular motions are likely responsible for the turbulence in the bottom waters, which produces a nepheloid layer about 100 km across, with a maximum thickness of about 600 m in water depths of 3100 m (Eittrheim et al., 1972).

8. Summary and conclusions

The study of existing cores collected across the Wilkes Land margin provides us with a previously unattainable age control (although low-resolution) for the Holocene and Pleistocene across the margin, which, in turn, allows us to calculate minimum sedimentation rates across the margin, and better understand the sediment distribution and processes across this margin during the Holocene and the Pleistocene glacial and interglacial cycles that could possibly be extended to the deeper unsampled sedimentary units imaged in reflection profiles. In summary, Holocene interglacial sedimentation is well represented in deep (> 1000 m) inner-shelf basins where diatomaceous ooze is deposited at estimated minimum sedimentation rates ranging from 40 to 60 cm/kyr. The quantitative diatom analyses show that the diatom species present in the core are indicative of

fluctuating sea-ice conditions with periodicities at the century scale.

Pleistocene *interglacial* sedimentation is well represented in sediment from the continental rise, and is dominated by hemipelagic deposition of massive mud with higher biogenic content, as indicated by high and contents and higher abundance of clasts. Pleistocene sedimentation during the *glacial* cycles is well represented across the margin and had been characterized by previous workers as dominated by diamictos on the continental shelf and turbidites and contourites on the continental rise. The main contribution of our study concerning Pleistocene glacial sedimentation in the studied margin sector is dominated by gravity flows. Slumps and/or the initial phase of a debris flow dominate the upper slope environment. Cores from the lower slope and upper continental rise contain crudely stratified to laminated intervals, which represent the transition between an end member of a debris flow and a turbidity flow. Some of the laminated intervals in cores from the continental rise represent sediment deposited from a turbidity flow. Other laminated sediments on the rise are the results of contourite deposition.

Acknowledgements

Our analyses of existing sediment cores from the Wilkes Land continental rise were possible with the support by the National Science Foundation grant #OPP-9815085, and by a grant from the Commission for Cultural, Educational and Scientific Exchange between the United States and Spain (Fulbright Program) GEMARANT Project# 99120. We thank Thomas Janecek and the staff at the Antarctic Research Facility in Florida State University and the USGS core repository in Menlo Park, California, where cores were examined and sampled. We thank Jim Channell for use of the paleomagnetism laboratory at University of Florida and the staff at the Institute of Rock Magnetism at University of Minnesota for assistance with the rock magnetic analyses. This manuscript was greatly improved thanks to

reviews by Xavier Crosta, Stephen Eittreim, and Monty Hampton.

References

- Acton, G.D., Guyodo, Y., Brachfeld, S.A., 2002. Magnetotratigraphy of sediment drifts on the continental rise of West Antarctica (ODP Leg 178, Sites 1095, 1096, and 1101). In: Barker, P.F., Camerlenghi, A., Acton, G.D., Ramsay, A.T.S. (Eds.), Proceedings ODP, Science Results, Vol. 178, 1–16 [CD-ROM].
- Anderson, J.B., 1999. Antarctic Marine Geology. Cambridge University Press, Cambridge, 289pp.
- Anderson, J.B., Kurtz, D.D., Weaver, F.M., 1979. Sedimentation on the Antarctic continental slope. In: Doyle, L.J., Pilkey, O. (Eds.), Geology of Continental Slopes, Soc. of Econ. Paleo. and Min., Special Publication No. 27, 127pp.
- Anderson, J.B., Kurtz, D.D., Domack, E.W., Balshaw, K.M., 1980. Glacial and glacial marine sediments of the Antarctic continental shelves. *Journal of Geology* 88, 399–414.
- Anderson, J.B., Brake, C., Domack, E.W., Myers, N., Singer, J., 1983. Sedimentary dynamics of the Antarctic continental shelf. In: Oliver, R.L., James, P.R., Jagob, J.B. (Eds.), Antarctic Earth Science. Cambridge University Press, New York, pp. 387–389.
- Barcena, M.A., Abrantes, F., 1998. Evidence of a high-productivity area off the coast of Málaga from studies of diatoms in surface sediments. *Marine Micropaleontology* 35, 91–103.
- Barcena, M.A., Gersonde, R., Ledesma, S., Fabres, J., Calafat, A.M., Canals, M., Sierro, F.J., Flores, J.A., 1998. Record of Holocene glacial oscillations in the Bransfield Basin as revealed by siliceous microfossil assemblages. *Antarctic Science* 10 (3), 269–285.
- Barcena, M.A., Isla, E., Plaza, A., Flores, J.A., Sierro, F.J., Masque, P., Sánchez-Cabeza, J.A., Palanques, A., 2002. Bioaccumulation record and paleoclimate significance in the western Bransfield Strait. The last 2000 yrs. *Deep-Sea Research II* 49, 935–950.
- Barker, P.F., Barrett, P., Camerlenghi, A., Cooper, A.K., Davey, Domack, E., Escutia, C., Jokat, W., O'Brien, P., 1998. Ice sheet history from Antarctic Continental margin sediments: the ANTOSTRAT approach. *Terra Antarctica* 5(4), 737–760.
- Barker, P.F., Camerlenghi, A., Acton, G.D., et al., 1999. Proceedings of the Ocean Drilling Program, Initial Reports, 178 [CD-ROM], ODP, College Station, Texas.
- Barnes, P.W., 1987. Morphologic Studies of the Wilkes land Continental Shelf, Antarctica-Glacial and Iceberg Effects. In: Eittreim, S.L., Hampton, M.A. (Eds.), The Antarctic Continental Margin: Geology and Geophysics of Offshore Wilkes Land: Circum-Pacific Council for Energy and Mineral Resources Earth Sciences Series, 5A. Houston, pp. 175–194.
- Barron, J., Larsen, B., Shipboard Scientific Party, 1991. Proceedings of the Ocean Drilling Program, Scientific Results, 119.
- Bartek, L.R., Vail, P.R., Anderson, J.B., Emmet, P.A., Wu, S., 1991. Effect of Cenozoic ice sheet fluctuations in Antarctica on the stratigraphic signature of the Neogene. *Journal of Geophysical Research* 96, 6753–6778.
- Burckle, L.H., Cooke, D.W., 1983. Late Pleistocene *Eucampia antarctica* abundance stratigraphy in the Atlantic sector of the Southern Ocean. *Micropaleontology* 29, 6–10.
- Cande, S.C., Mutter, J.C., 1982. A revised identification of the oldest sea-floor spreading anomalies between Australia and Antarctica. *Earth and planetary Science Letters* 58, 151–160.
- Censarek, B., Gersonde, R., 2002. Miocene diatom biostratigraphy at ODP sites 689, 690, 1088, 1092 (Atlantic sector of the Southern Ocean). *Marine Micropaleontology* 45 (3–4), 309–356.
- Chase T. E., Seekins, B.A., Young, J.D., Eittreim, S.L., 1987. Marine topography of offshore Antarctica. In: Eittreim, S.L., Hampton, M.A. (Eds.), The Antarctic Continental Margin: Geology and Geophysics of Offshore Wilkes Land: Circum-Pacific Council for Energy and Mineral Resources Earth Sciences Series, 5A, Houston, pp. 147–150.
- Cooper, A.K., Barret, P.J., Hinz, K., Traube, V., Leitchenkov, G., Stagg, H.M.J., 1991. Cenozoic prograding sequences of the Antarctic continental margin: A record of glacioeustatic and tectonic events. *Marine Geology* 102, 175–213.
- Crowley, T.J., North, G.R., 1977. Pleoclimatology. Oxford University Press, Inc., Oxford, 349pp.
- Day, R., Fuller, M., Schmidt, V.A., 1977. Hysteresis properties of titanomagnetites: Grainsize and compositional dependence. *Physics of the Earth and Planetary Interiors* 13, 260–267.
- Domack, E.W., 1982. Sedimentology of glacial and glacial marine deposits on the George V Adélie continental shelf, East Antarctica. *Boreas* 11, 79–97.
- Domack, E.W., Anderson, J.B., 1983. Marine Geology of the George V continental margin: combined results of Deep Freeze 79 and the 1911–14 Australasian expedition. In: Oliver, R.L., James, P.R., Jago, J.B. (Eds.), Antarctic Earth Science. Cambridge University Press, New York, pp. 402–406.
- Domack, E.W., Jull, A.J.T., Anderson, J.B., Linick, T.W., Williams, C.R., 1989. Application of tandem accelerator mass-spectrometer dating to late Pleistocene-Holocene sediments of the East Antarctic continental shelf. *Quaternary Research* 31, 277–287.
- Domack, E.W., Mashiotto, T.A., Burkley, L.A., Ishman, S.E., 1993. 300-year cyclicity in organic matter preservation in Antarctic fjord sediments. In: Kennett, J.P., Warnke, D.A. (Eds.), The Antarctic Paleoenvironment: A perspective on Global Change, Vol. 60 (Part 2), pp. 265–272.
- Dreimanis, A., Goldthwait, R.P., 1973. Wisconsin glaciation in the Huron, Erie and Ontario lobes. In: Black, R.F., et al. (Eds.), The Wisconsinian Stage, Vol. 136, Geological Society of American Members, pp. 71–106.

- Drewry, D.J., Cooper, A.P.R., 1981. Processes and models of Antarctic glaciomarine sedimentation. *Annals of Glaciology* 2, 117–122.
- Dunbar, R.B., Anderson, J.B., Domack, E.W., 1985. Oceanographic influences on sedimentation along the Antarctic continental shelf. In: Jacobs, S.S. (Ed.), *Oceanology of the Antarctic Continental Shelf*. Antarctic Research Series 43, American Geophysical Union Washington, DC, pp. 291–312.
- Eittrreim, S.L., 1994. Transition from continental to oceanic crust on the Wilkes-Adélie margin of Antarctica. *Journal of Geophysical Research* 99, 24189–24205.
- Eittrreim, S.L., Smith, G.L., 1987. Seismic sequences and their distribution on the Wilkes Land margin. In: Eittrreim, S.L., Hampton, M.A. (Eds.), *The Antarctic Continental Margin: Geology and Geophysics of Offshore Wilkes Land: Circum-Pacific Council for Energy and Mineral Resources Earth Sciences Series, 5A*, Houston, pp. 15–43.
- Eittrreim, S.L., Bruchhausen, P.M., Ewing, M., 1972. Vertical distribution of turbidity in the south Indian and south Australian basins, in: Hayes, D.E., ed., *Antarctic Oceanology II. The Australian-New Zealand Sector*. Antarctic Research Series, v. 19. p. 51–58.
- Eittrreim, S.L., Cooper, A.K., Wannesson, J., 1995. Seismic stratigraphic evidence of icesheet advances on the Wilkes Land margin of Antarctica. *Sedimentary Geology* 96, 131–156.
- Escutia, C., Eittrreim, S.L., Cooper, A.K., 1997. Cenozoic glaciomarine sequences on the Wilkes Land continental rise, Antarctica: Proceedings, Vol. VII. International Symposium on Antarctic Earth Sciences, pp. 791–795.
- Eittrreim, S.L., Gordon, A.L., Ewing, M., Thorndike, E.M., Bruchhausen, P.M., 1971. The nepheloid layer and observed bottom currents in the Indian-Pacific Antarctic Sea, in: *Studies in Physical Oceanography—A tribute to George Wüst on his 80th birthday* (A.L. Gordon ed.). Gordon and Breach, New York, p. 19–35.
- Escutia, C., Eittrreim, S.L., Cooper, A.K., Nelson, C.H., 2000. Morphology and acoustic character of the Antarctic Wilkes Land turbidite systems: Ice-sheet sourced versus riversourced fans. *Journal of Sedimentary Research* 70 (1), 84–93.
- Escutia, C., Nelson, C.H., Acton, G.D., Cooper, A.K., Eittrreim, S.L., Warnke, D.A., Jaramillo, J., 2002. Current controlled deposition on the Wilkes Land continental rise. In: Stow, D., et al. (Eds.), *Deep-Water Contourite Systems: Modern Drifts and Ancient Series, Seismic and Sedimentary Characteristics*. The Geological Society of London, Memoirs 22, 373–378.
- Gersonde, R., Barcena, M.A., 1998. Revision of the upper Pliocene–Pleistocene diatom biostratigraphy for the northern belt of the Southern Ocean. *Micropaleontology* 44 (1), 84–98.
- Gersonde, R., Abelmann, A., Burckle, L.H., Hamilton, N., Lazarus, D., McCartney, K., O'Brien, P., Spiess, V., Wise, Jr., S.W., 1990. Biostratigraphic synthesis of Neogene siliceous microfossils from the Antarctic Ocean, ODP Leg 113 (Weddell Sea). Proceedings of Ocean Drilling Program, Scientific Results, Vol. 113, pp. 915–936.
- Gordon, A.L., Tchernia, P., 1972. Waters of the continental margin off the Adélie Coast, Antarctica. In: Hayes, D.E. (Ed.), *Antarctic Oceanology II. The Australian-New Zealand Sector*. Antarctic Research Series, Vol. 19, pp. 59–70.
- Guyodo, Y., Acton, G.D., Brachfeld, S., Channell, J.E.T., 2001. A sedimentary paleomagnetic record of the Matuyama Chron from the western Antarctic margin (ODP Site 1101). *Earth Planetary Science Letters* 191, 61–74.
- Hampton, M.A., 1972. The role of subaqueous debris flows in generating turbidity currents. *Journal of Sedimentary Petrology* 42, 775–793.
- Hampton, M.A., Eittrreim, S.L., Richmond, B.M., 1987a. Post-breakup sedimentation on the Wilkes Land Margin, Antarctica. In: Eittrreim, S.L., Hampton, M.A. (Eds.), *The Antarctic Continental Margin: Geology and Geophysics of Offshore Wilkes Land: Circum-Pacific Council for Energy and Mineral Resources Earth Sciences Series, 5A*, Houston, pp. 75–88.
- Hampton, M.A., Eittrreim, S.L., Richmond, B.M., 1987b. Geology of sediment cores from the George V continental margin. In: Eittrreim, S.L., Hampton, M.A. (Eds.), *The Antarctic Continental Margin: Geology and Geophysics of Offshore Wilkes Land: Circum-Pacific Council for Energy and Mineral Resources Earth Sciences Series, 5A*, Houston, pp. 75–88.
- Hayes, D.E., Frakes, L.A., et al., 1975. Initial Reports of the Deep Sea Drilling Project, 28, Washington (US Government Printing Office).
- Kennett, J.P., Hodell, D.A., 1993. Evidence for relative climatic stability of Antarctica during the early Pliocene: A marine perspective. *Geografiska Annaler* 75A, 205–220.
- Kirschvink, J.L., 1980. The least-squares line and plane and the analysis of palaeomagnetic data. *Geophysical Journal of the Royal Astronomical Society* 62, 699–718.
- Kuvaas, B., Kristoffersen, Y., 1991. The Crary Fan: A trough-mouth fan on the Weddell sea continental margin. Antarctica: Marine Geology 97, 345–362.
- Labeyrie, L.D., et al., 1986. Melting history of Antarctica during the past 60,000 years. *Nature* 322, 701–706.
- Labracherie, M., et al., 1989. The last deglaciation in the Southern Ocean. *Paleoceanography* 4, 629–638.
- Larter, R.D., Barker, P.F., 1989. Neogene interaction of tectonic and glacial processes at the Pacific margin of the Antarctic Peninsula. In: McDonald, D.I.M. (Ed.), *Sedimentation, Tectonics and Eustasy*. International Association of Sedimentologists, Special Publication 12, Blackwell, Oxford, pp. 165–186.
- Leventer, A., Domack, E., Ishman, S.E., Brachfeld, S., McClennen, C.E., Manley, P., 1996. Productivity cycles of 200–300 years in the Antarctic Peninsula region: understanding linkages among the sun, atmosphere, oceans, Sea Ice, and Biota. *Geological Society of American Bulletin* 108 (12), 1626–1644.

- Lindstrom, D., Tyler, D., 1984. Preliminary results of Pine Island and Thwaites Glaciers study. *Antarctica Journal of US* 19, 53–55.
- Lowrie, W., Fuller, M., 1971. On the alternating field demagnetization characteristics of multidomain thermoremanent magnetization in magnetite. *Journal of Geophysical Research* 76, 6339–6349.
- MacDonald, T.R., Ferrigno, J.G., Williams Jr, R.S., Lucchitta, B.K., 1989. Velocities of Antarctic outlet glaciers determined from sequential Landsat images. *Antarctica Journal of US* 24, 105–106.
- Milam, R.W., Anderson, J.B., 1981. Distribution and ecology of recent benthonic foraminifera of the Adélie-George V continental shelf and slope, Antarctica. *Marine Micropaleontology* 6, 297–325.
- Mortlock, R.A., Froelich, P.N., 1989. A simple method for the rapid determination of biogenic opal in pelagic marine sediments. *Deep-Sea Research* 36 (9), 1415–1426.
- O'Brien, P.E., Cooper, A.K., Richter, C., et al., 2001. Proceedings of the Ocean Drilling Program, Initial Reports, 188 [CD-ROM], ODP, College Station, Texas.
- Payne, R.R., Conolly, J.R., 1972. Turbidite sedimentation off the Antarctic continent. *Antarctic Research Series* 19, 349–364.
- Presti, M., Armand, L., Brambati, A., Buseti, M., De Santis, L., Harris, P., 2001. Evolution of Mertz Drift (George V Basin, East Antarctica) during the Late Pleistocene-Holocene. Project WEGA, PNRA-Australian Antarctic Division, Wilkes Basin Glacial History (East Antarctica), 2nd Workshop, Trieste, August 27–31, 2001.
- Schrader, H.J., Gersonde, R., 1978. Diatoms and silicoflagellates. In: Zachariasse, W.J., et al. (Eds.), *Micropaleontological Counting Methods and Techniques—an exercise on an eight metres section of the Lower Pliocene of Capo Rossello, Sicily*. Utrecht Micropaleontological Bulletin 17, pp. 129–176.
- Shipboard Scientific Party, 2001. Leg 188 summary: Prydz Bay-Cooperation Sea, Antarctica. In: O'Brien, P.E., Cooper, A.K., Richter, C., et al. (Eds.), *Proceedings of ODP, Initial Reports, 188*, College Station, TX (Ocean Drilling Program), pp. 1–65.
- Tanahashi, M., Eittrheim, S., Wannesson, J., 1994. Seismic stratigraphic sequences of the Wilkes Land margin. *Terra Antarctica* 1 (2), 391–393.
- Veevers, J.J., 1987. The conjugate continental margin of Antarctica and Australia. In: Eittrheim, S.L., Hampton, M.A. (Eds.), *The Antarctic Continental Margin: Geology and Geophysics of Offshore Wilkes Land: Circum-Pacific Council for Energy and Mineral Resources Earth Sciences Series, 5A*, Houston, pp. 45–74.
- Wannesson, J., 1991. Geology and petroleum potential of the Adélie Coast margin, East Antarctica. In: St. John, B. (Ed.), *Antarctica as an Exploration Frontier: American Association of Petroleum Geologists, Studies in Geology # 31*, pp. 77–87.
- Watkins, N.D., Kennett, J.P., 1972. Regional sedimentary discontinuities and upper Cenozoic changes in bottom water velocities between Australia and Antarctica. In: Hayes, D.E. (Ed.), *Antarctic Oceanology II. The Australian-New Zealand Sector*. Antarctic Research Series 19, pp. 273–294.
- Warnke, D.A., Allen, C.P., Muller, D.W., Hodell, D.A., Brunner, C.A., 1992. Miocene-Pliocene Antarctic glacial evolution: A synthesis of ice-rafted debris, stable isotope, and planktonic foraminiferal indicators, ODP leg 114. The Antarctic Paleoenvironment a perspective in global change. *Antarctic Research Series* 56, pp. 311–325.
- Zielinski, U., Gersonde, R., 2002. Plio-pleistocene diatom biostratigraphy from ODP Leg 177, Atlantic sector of the southern ocean. *Marine Micropaleontology* 45 (3–4), 225–268.